Electronic Supporting Information for:

Synthesis, Conformational Analysis and Antimicrobial Activity of Au(I)-Ag(I) and Au(I)-Hg(II) Heterobimetallic *N*-Heterocyclic Carbene Complexes

Zili Li,[a] Emily R. R. Mackie,[b] Pria Ramkissoon,[a] Joel C. Mather,[a] Nutchareenat Wiratpruk,[a] Tatiana Soares da Costa[b] and Peter J. Barnard[a]*

[a]Department of Chemistry and Physics, La Trobe Institute for Molecular Science, La Trobe University, Victoria, 3086, Australia, E-mail: p.barnard@latrobe.edu.au.
[b]Department of Biochemistry and Genetics, La Trobe Institute for Molecular Science, La Trobe University Victoria 3086, Australia.

Synthesis

1. A mixture of imidazole (10.00 g, 146.89 mmol), finely powdered KOH (9.88 g, 176.26 mmol) and *tetra-n*-butylammonium bromide (1.42 g, 4.41 mmol) was stirred at RT for 1 h followed by addition of dibromomethane (5.10 mL, 73.44 mmol). The resultant mixture was heated to 40 °C for 24 h followed by the addition of finely powdered KOH (4.94 g, 88.13 mmol) and dibromomethane (5.10 mL, 73.44 mmol). After 24 h the mixture was extracted with chloroform (5 × 20 mL) and the combined organic fractions were concentrated to 20 mL *in vacuo* followed by the addition of hexane (5 mL) to obtain a pale yellow crystalline solid. Yield: 1.45 g, 13.3 %. ^{1}H-NMR (500.023 MHz, d$_6$-DMSO): δ = 7.93 (s, 2H, *H*$_{imi}$), 7.40 (s, 2H, *H*$_{imi}$), 6.91 (s, 2H, *H*$_{imi}$), 6.22 (s, 2H, C*H*$_2$). ^{13}C-NMR (125.74 MHz, d$_6$-DMSO): δ = 137.7 (*C*$_{imi}$), 129.6 (*C*$_{imi}$), 119.5 (*C*$_{imi}$), 55.2 (*C*H$_2$). ESI-MS$^+$: [C$_7$H$_9$N$_4$]$^+$ *m/z* = 149.19, calcd = 149.18.

7. This compound was prepared according to a literature procedure.[1] A solution of *N*-ethylimidazole (2.00 g, 20.80mmol) and diiodomethane (0.93 mL, 11.44 mmol) in THF (20 mL) was stirred at reflux for 2 d. The resultant solid was collected and washed with THF (3 × 5 mL) and acetonitrile (5 mL) and dried *in vacuo* yielding the product as an off-white powder. Yield: 1.78 g, 37.2%. ^{1}H-NMR (500.023 MHz, d$_6$-DMSO): δ = 9.46 (s, 2H, *H*$_{imi}$), 8.01 (t, $^{3}J_{H\text{-}H}$ = 1.9 Hz, 2H, *H*$_{imi}$), 7.93 (t, $^{3}J_{H\text{-}H}$ = 1.7 Hz, 2H, *H*$_{imi}$), 6.64 (s, 2H, C*H*$_2$), 4.27 (q, $^{3}J_{H\text{-}H}$ = 7.3 Hz, 4H, C*H*$_2$CH$_3$), 1.45 (t, $^{3}J_{H\text{-}H}$ = 7.3 Hz, 6H, CH$_2$C*H*$_3$). ^{13}C-NMR (125.74 MHz, d$_6$-DMSO): δ = 137.7 (*C*$_{imi}$), 123.3 (*C*$_{imi}$), 122.6 (*C*$_{imi}$), 58.7 (*C*H$_2$), 45.2 (*C*H$_2$CH$_3$), 15.2 (CH$_2$*C*H$_3$). ESI-MS$^+$: [C$_{11}$H$_{18}$N$_4$I]$^+$ *m/z* = 333.00, calcd = 333.06, [C$_{11}$H$_{18}$N$_4$]$^{2+}$ *m/z* = 103.20, calcd = 103.57.

8a. This compound was prepared according to a literature procedure[2] from **7** (0.10 g, 0.22 mmol), (THT)AuCl (0.070 g, 0.22 mmol), NaOAc (0.036 g, 0.44 mmol) and KBF$_4$ (0.041 g, 0.33 mmol).

Yield: 0.072 g, 30.3%. ^{1}H-NMR (500.023 MHz, d$_6$-DMSO): δ = 7.89 (d, J = 1.7 Hz, 4H, H_{imi}), 7.71 (d, $^{3}J_{H\text{-}H}$ = 1.8 Hz, 4H, H_{imi}), 7.14 (d, $^{3}J_{H\text{-}H}$ = 13.9 Hz, 2H, CH_2), 6.35 (d, $^{3}J_{H\text{-}H}$ = 14.0 Hz, 2H, CH_2), 4.10 – 4.40 (m, 8H, CH_2CH$_3$), 1.40 (t, $^{3}J_{H\text{-}H}$ = 7.3 Hz, 12H, CH$_2$CH_3). ^{13}C-NMR (125.74 MHz, d$_6$-DMSO): δ = 182. 7 ($C_{carbene}$), 123. 5 (C_{imi}), 122.4 (C_{imi}), 62.6 (CH$_2$), 46.7 (CH$_2$CH$_3$), 17.1 (CH$_2$$CH_3$). ESI-MS$^+$: [C$_{22}H_{32}N_8Au_2BF_4$]$^+$ *m/z* = 889.20, calcd = 889.21, [C$_{22}$H$_{32}$N$_8$Au$_2$]$^{2+}$ *m/z* = 401.20, calcd = 401.10.

8b. This compound was prepared according to a literature procedure.[1] A mixture of **7** (0.10 g, 0.22 mmol) and Ag$_2$O (0.13 g, 0.55 mmol) in water (5 mL) was stirred at RT in the absence of light for 1 h and then filtered through a plug of Celite. To the filtrate was added a saturated aqueous solution of KBF$_4$ (10 mL) and the resultant precipitate was collected and washed with water (2 × 5 mL), isopropanol (5 mL) and diethyl ether (5 mL), yielding the product as a white powder. Yield: 0.050 g, 25.2%. ^{1}H-NMR (500.023 MHz, d$_6$-DMSO): δ = 7.88 (d, $^{3}J_{H\text{-}H}$ = 1.1 Hz, 4H, H_{imi}), 7.65 (d, $^{3}J_{H\text{-}H}$ = 1.1 Hz, 4H, H_{imi}), 6.70 – 7.15 (m, 2H, CH_2), 6.25 – 6.70 (m, 2H, CH_2), 4.19 (q, $^{3}J_{H\text{-}H}$ = 7.2 Hz, 8H, CH_2CH$_3$), 1.37 (t, $^{3}J_{H\text{-}H}$ = 7.3 Hz, 12H, CH$_2$CH_3). ^{13}C-NMR (125.74 MHz, d$_6$-DMSO): δ = 206.9 ($C_{carbene}$), 123.1 (C_{imi}), 122.3 (C_{imi}), 47.1 (CH$_2$), 31.3 (CH$_2$CH$_3$), 17.4 (CH$_2$$CH_3$). ESI-MS$^+$: [C$_{22}H_{32}N_8Ag_2BF_4$]$^+$ *m/z* = 711.20, calcd = 889.21, [C$_{22}$H$_{32}$N$_8$Au$_2$]$^{2+}$ *m/z* = 311.20, calcd = 311.04.

9. This compound was prepared using the same method as described for **1** using imidazole (5.44 g, 80.00 mmol), 1,2-dichloroethane (6.36 mL, 80.32 mmol), KOH (8.04 g, 143.28 mmol) and *tetra-n*-butylammonium bromide (0.76 g, 2.36 mmol). Yield: 2.44 g, 34.6 %. ^{1}H-NMR (500.023 MHz, d$_6$-DMSO): δ = 7.37 (s, 2H, H_{imi}), 7.00 (s, 2H, H_{imi}), 6.85 (s, 2H, H_{imi}), 4.32 (s, 4H, CH_2). ^{13}C-NMR (125.74 MHz, d$_6$-DMSO): δ = 137.8 (C_{imi}), 129.0 (C_{imi}), 119.5 (C_{imi}), 47.1 (CH$_2$). HRESI-MS$^+$: [C$_8$H$_{11}$N$_4$]$^+$ *m/z* = 163.0930, calcd = 163.0984.

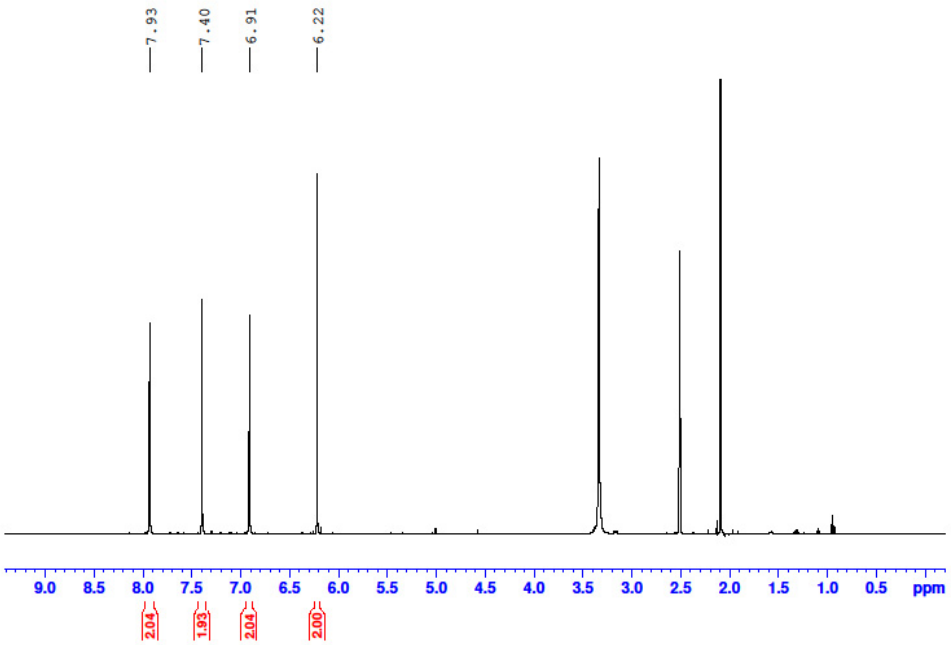

Figure S1. ^{1}H-NMR spectrum of compound **1**.

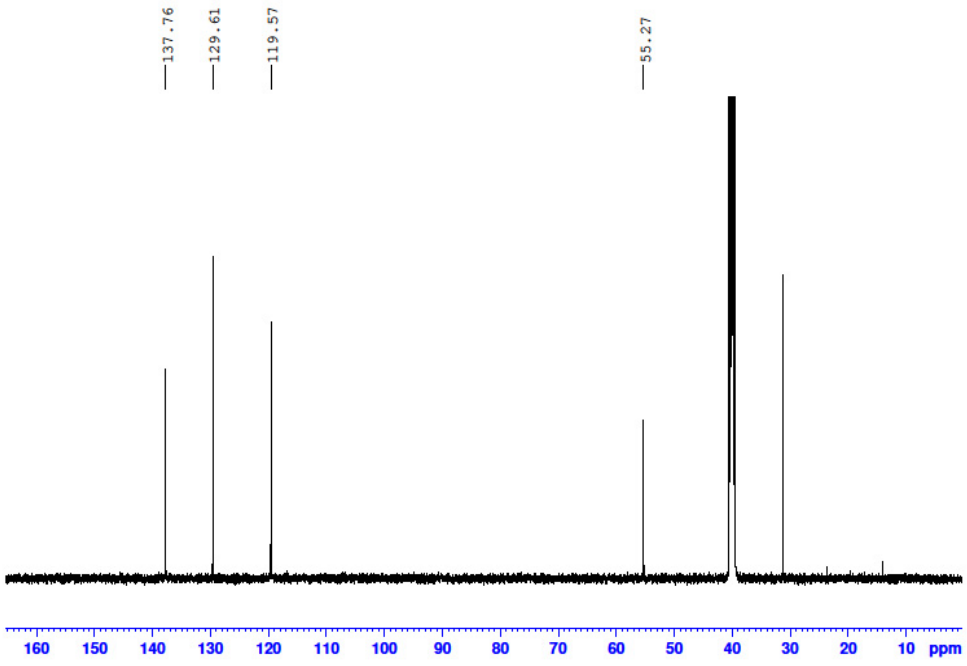

Figure S2. ^{13}C-NMR spectrum of compound **1**.

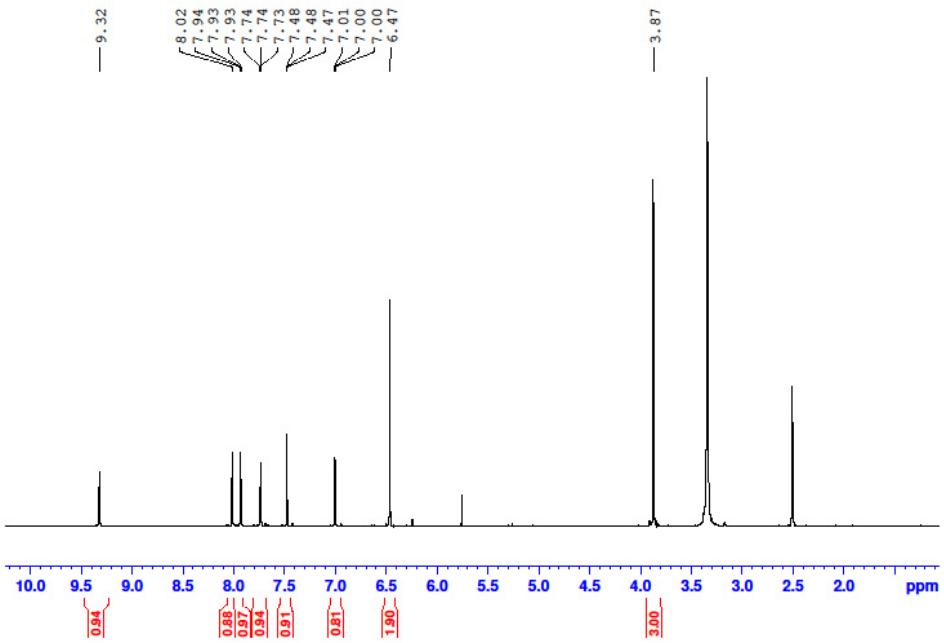

Figure S3. [1]H-NMR spectrum of pro-ligand **2a**.

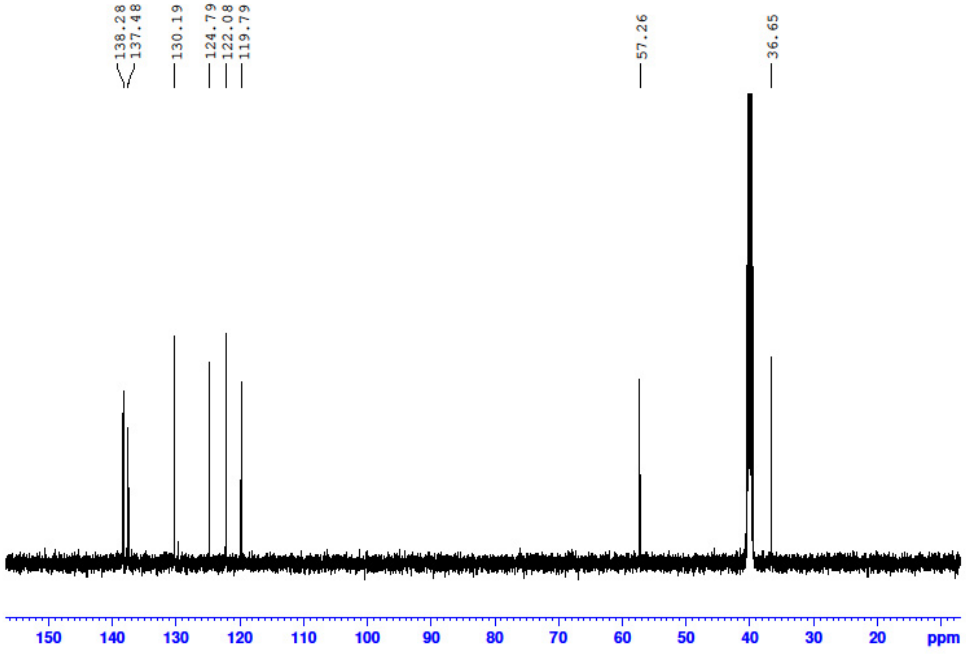

Figure S4. [13]C-NMR spectrum of pro-ligand **2a**.

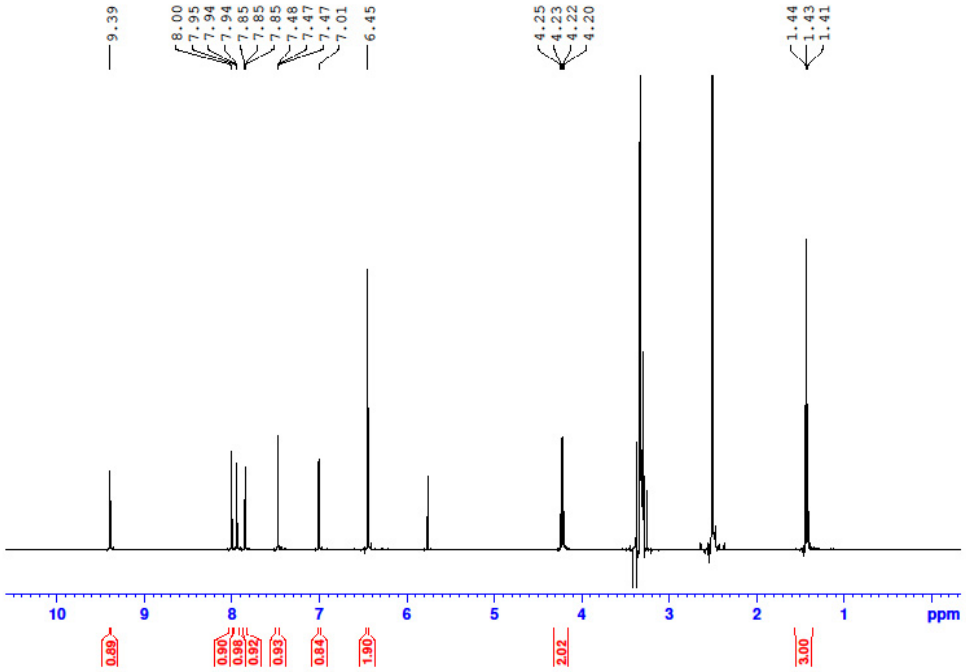

Figure S5. ^{1}H-NMR spectrum of pro-ligand **2b**.

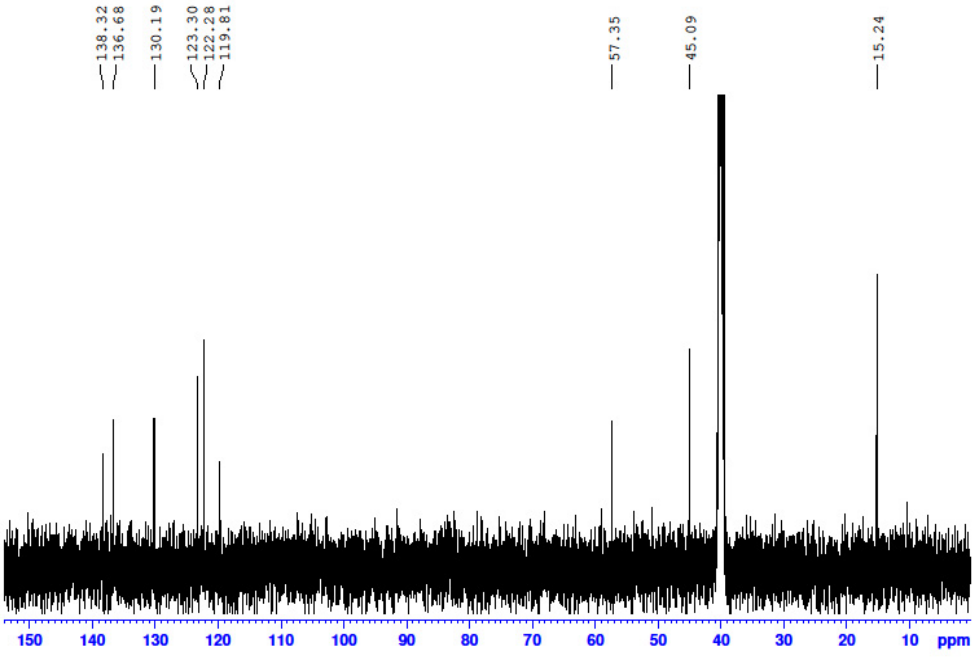

Figure S6. ^{13}C-NMR spectrum of pro-ligand **2b**.

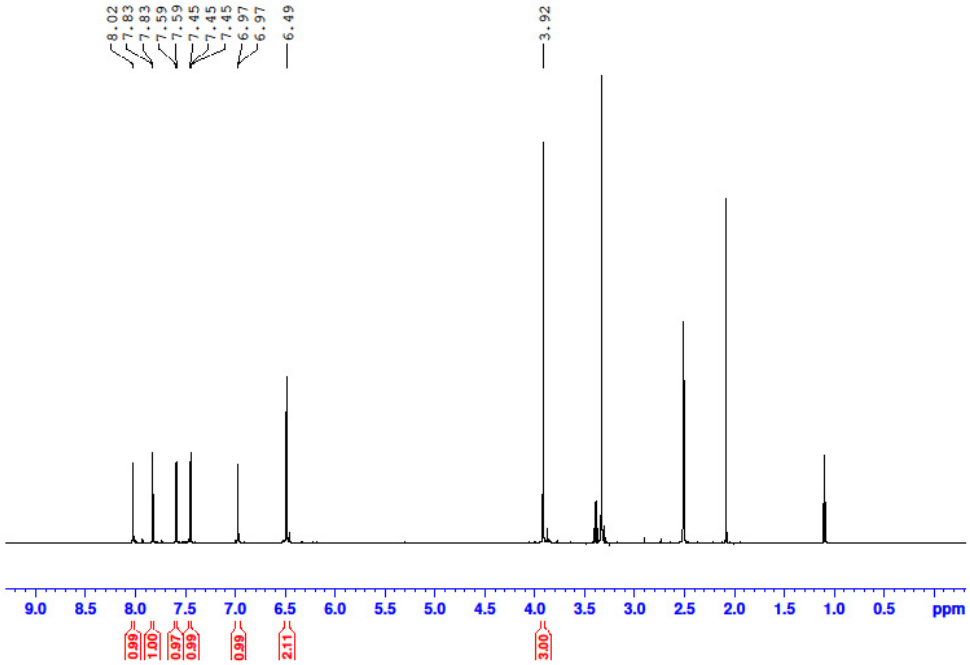

Figure S7. ^{1}H-NMR spectrum of Au(I) monometallic complex **3a**.

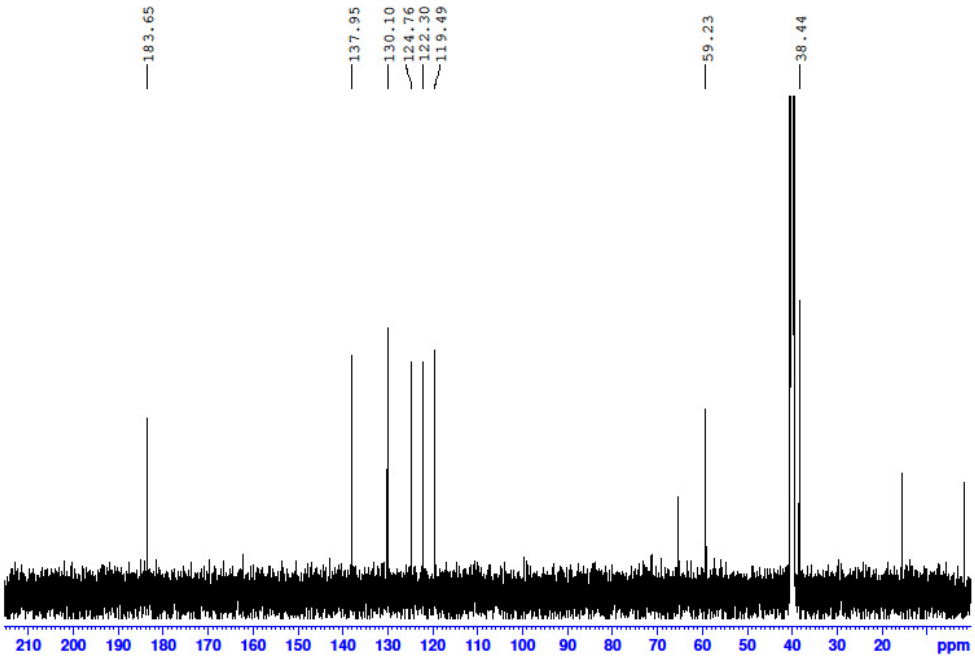

Figure S8. ^{13}C-NMR spectrum of Au(I) monometallic complex **3a**.

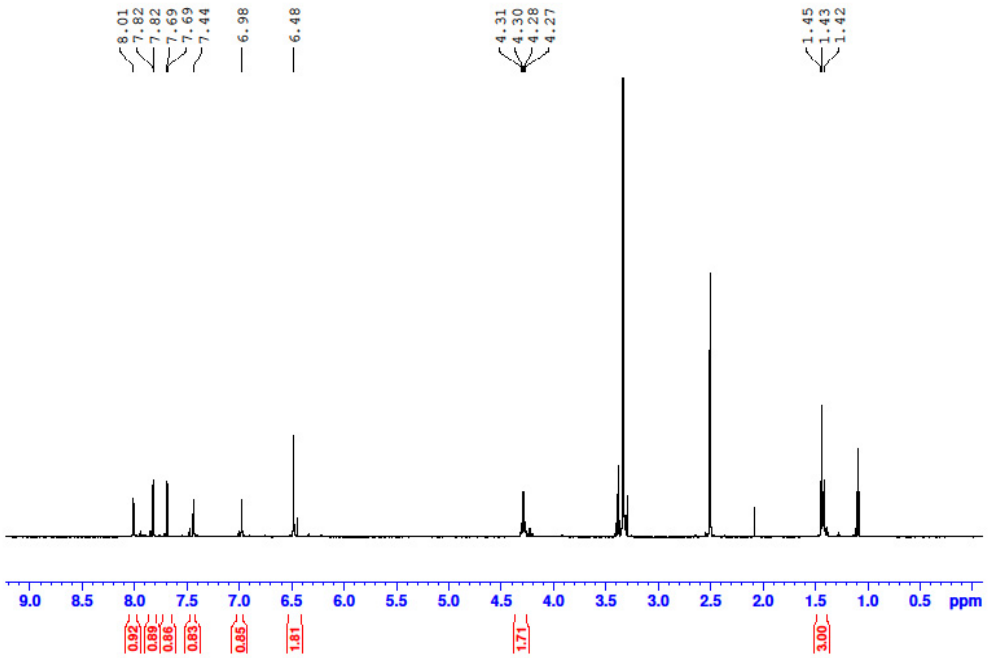

Figure S9. [1]H-NMR spectrum of Au(I) monometallic complex **3b**.

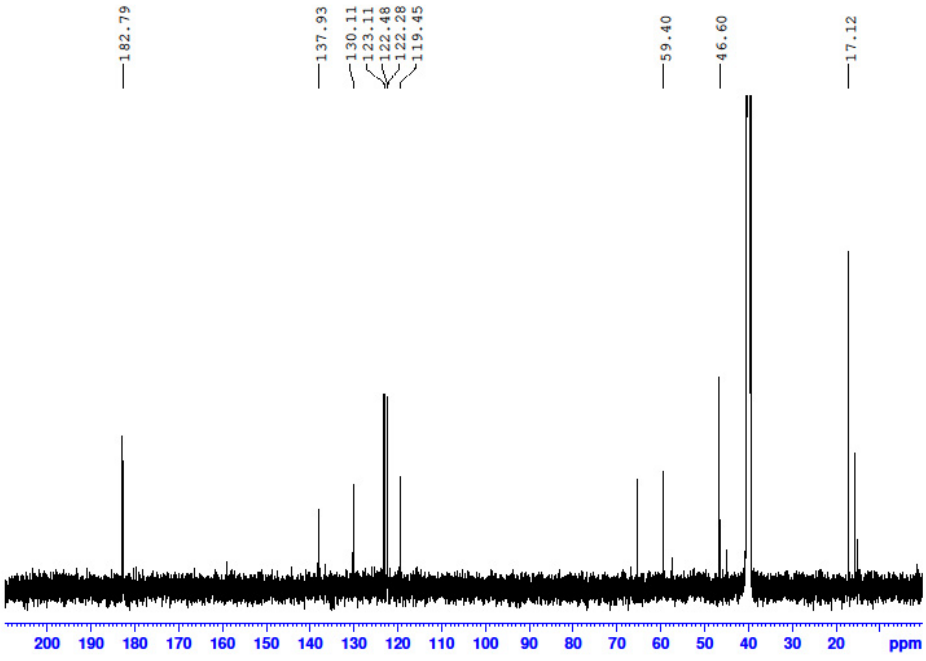

Figure S10. [13]C-NMR spectrum of Au(I) monometallic complex **3b**.

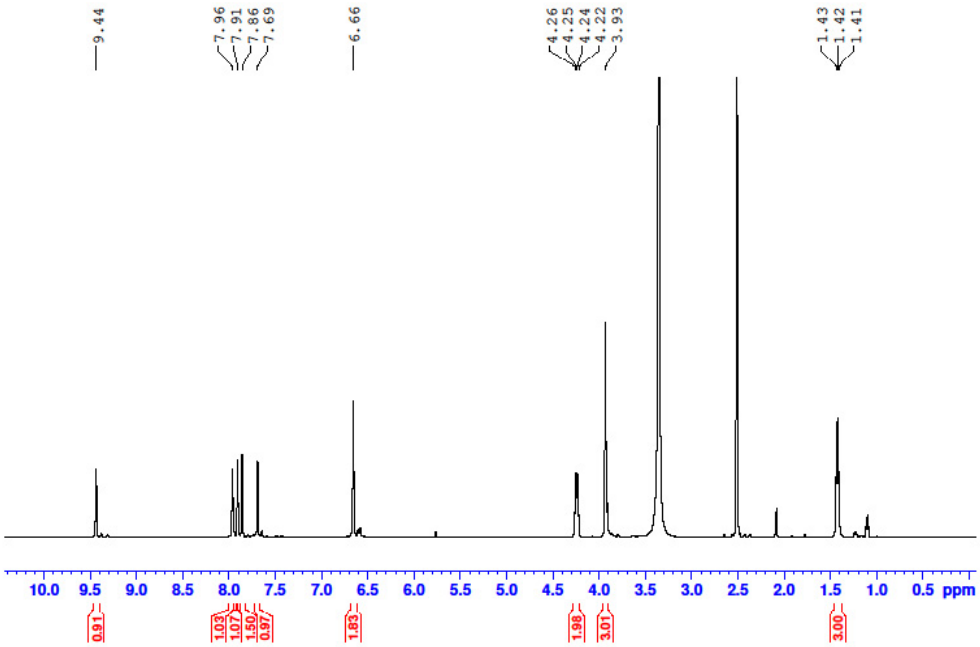

Figure S11. ^{1}H-NMR spectrum of Au(I) monometallic complex **4a**.

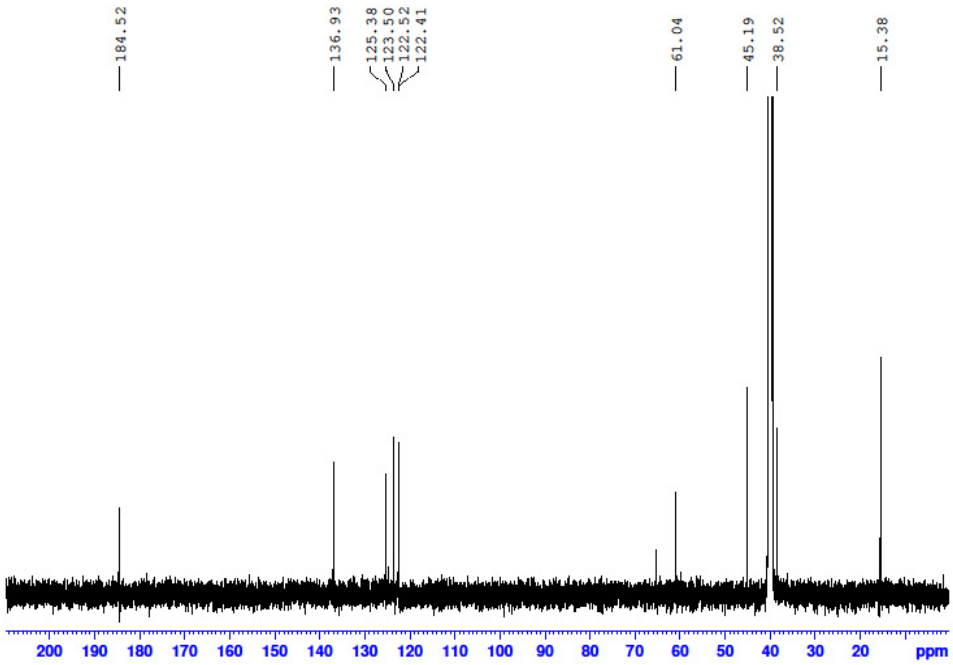

Figure S12. ^{13}C-NMR spectrum of Au(I) monometallic complex **4a**.

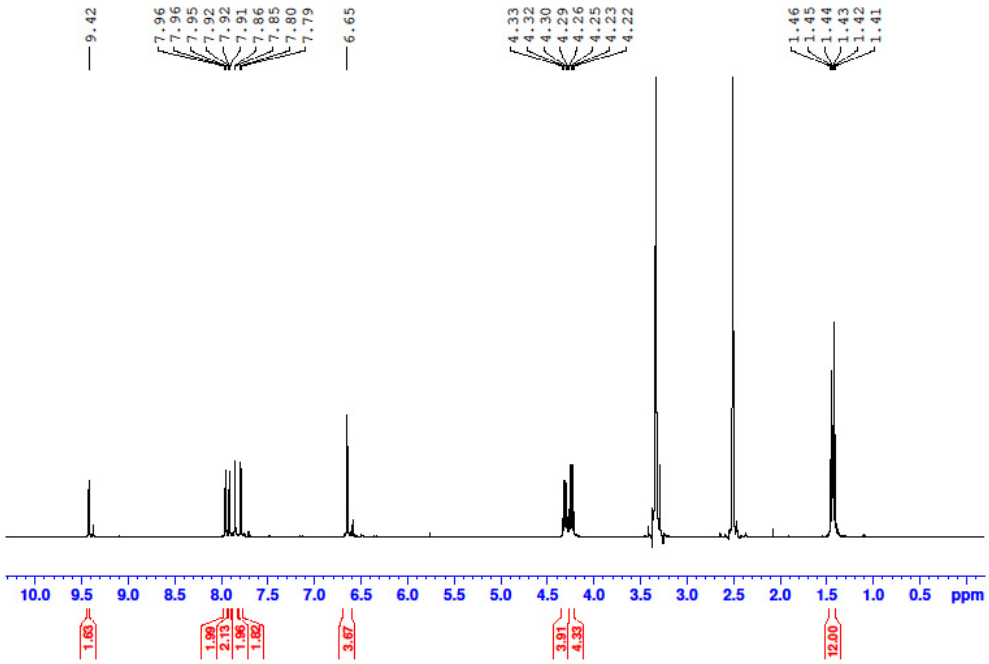

Figure S13. ^{1}H-NMR spectrum of Au(I) monometallic complex **4b**.

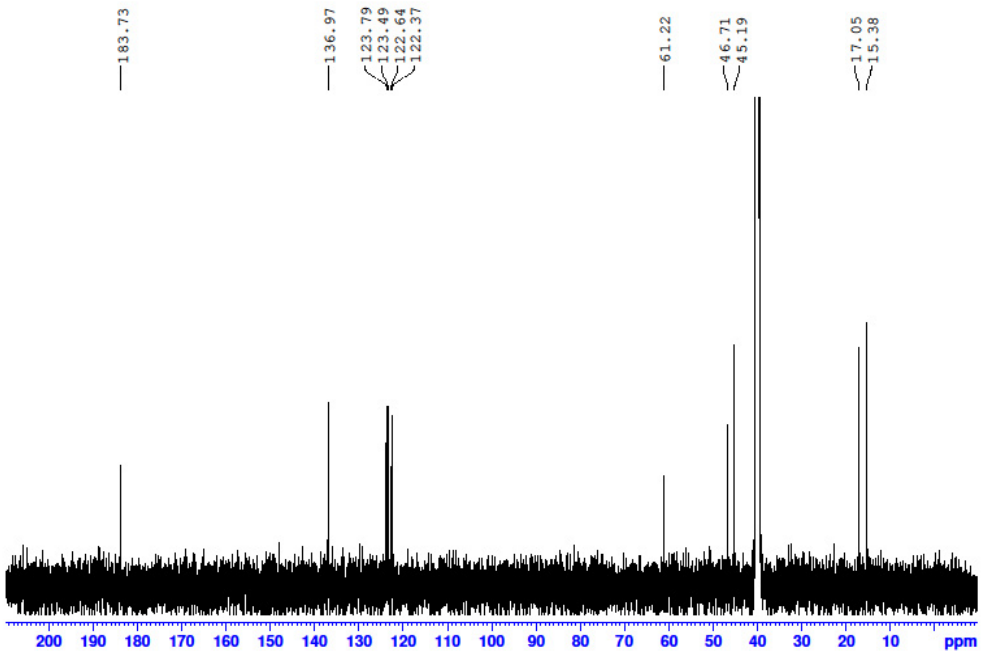

Figure S14. ^{13}C-NMR spectrum of Au(I) monometallic complex **4b**.

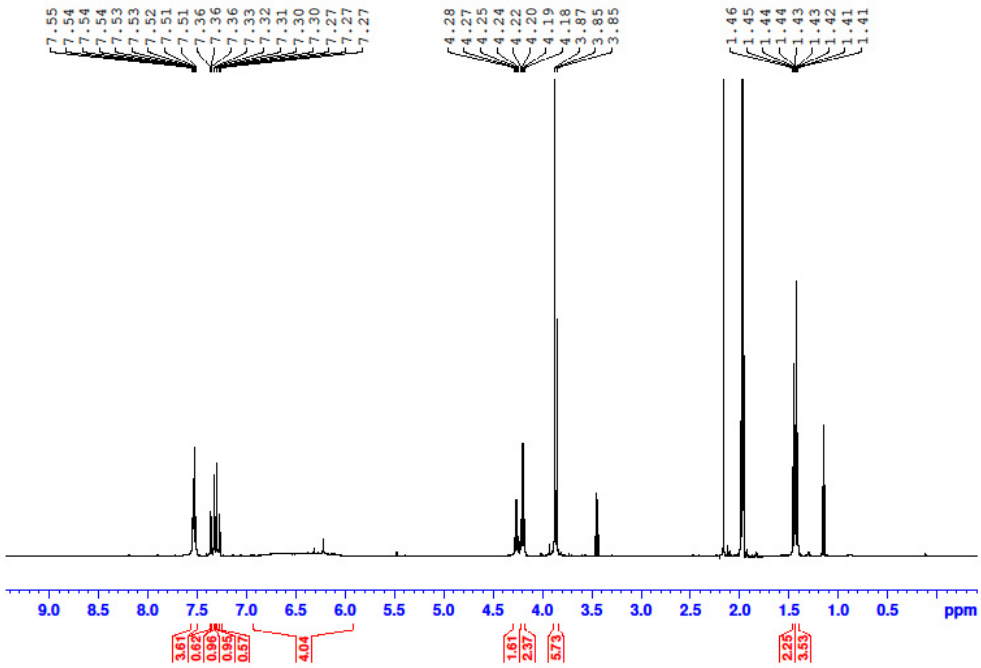

Figure S15. ^{1}H-NMR spectrum of Au(I)-Ag(I) heterobimetallic complex **5a**.

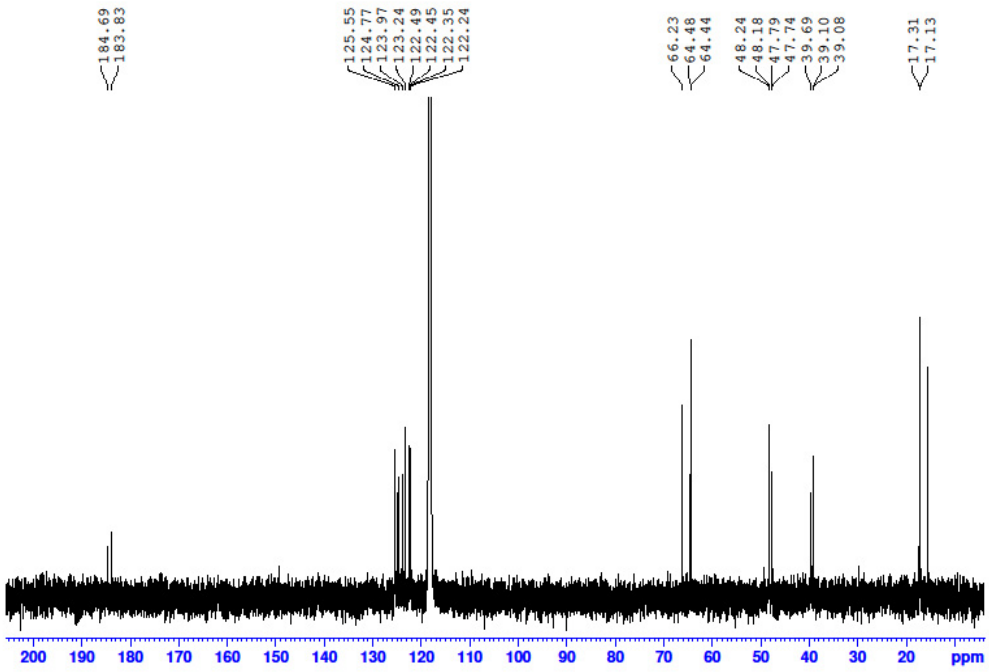

Figure S16. ^{13}C-NMR spectrum of Au(I)-Ag(I) heterobimetallic complex **5a**.

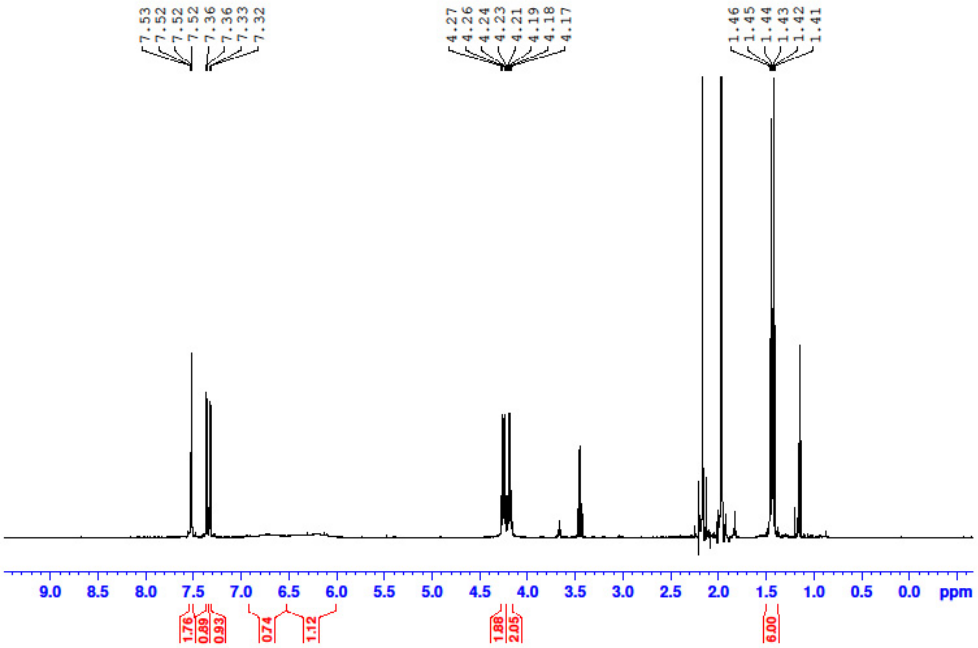

Figure S17. ^{1}H-NMR spectrum of Au(I)-Ag(I) heterobimetallic complex **5b**.

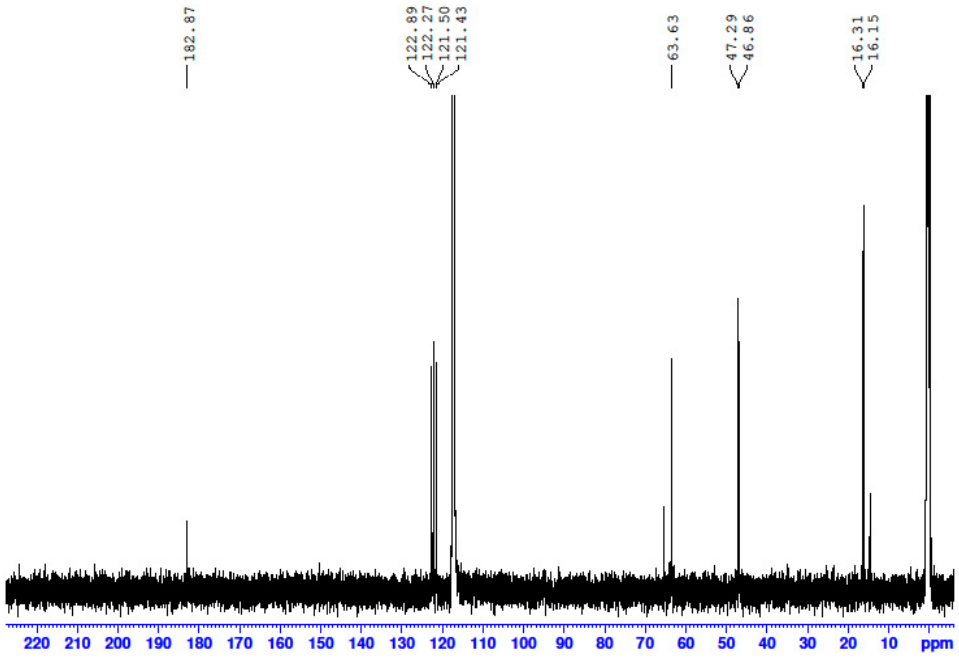

Figure S18. ^{13}C-NMR spectrum of Au(I)-Ag(I) heterobimetallic complex **5b**.

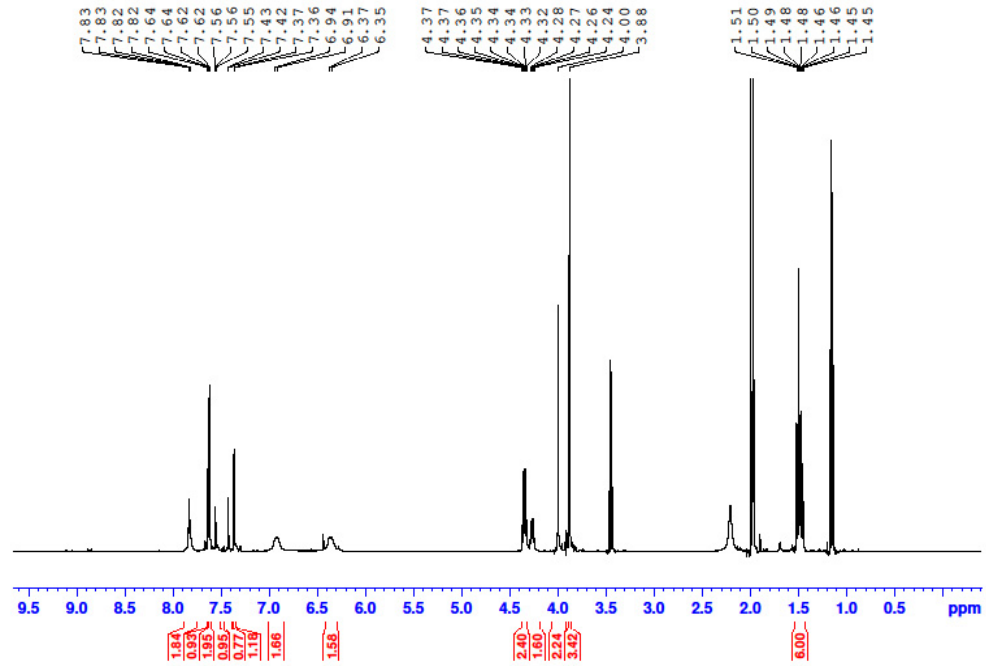

Figure S19. ^{1}H-NMR spectrum of Au(I)-Hg(II) heterobimetallic complex **6a**.

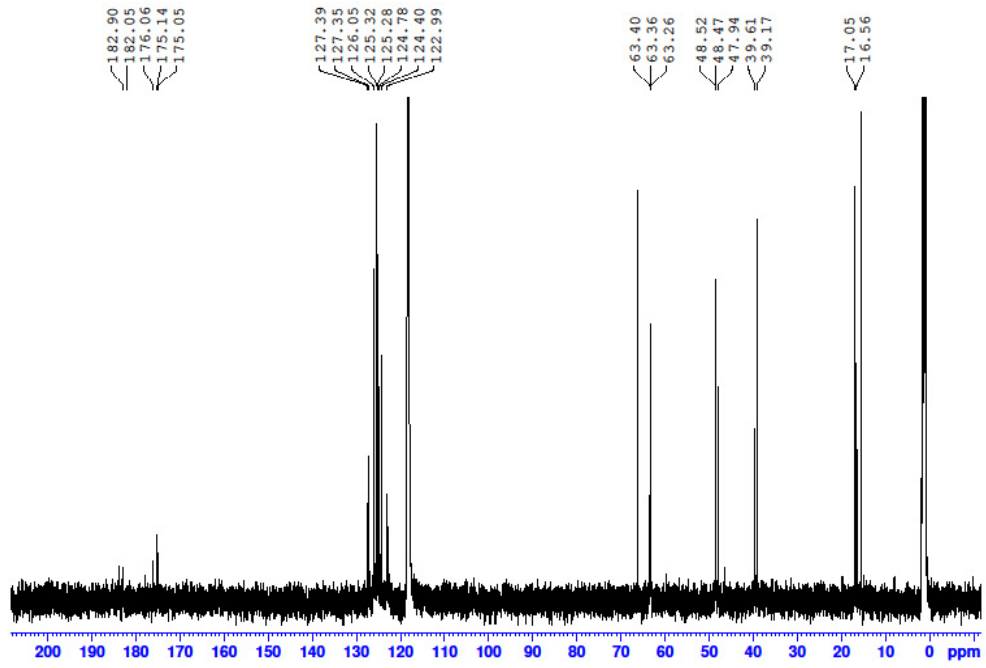

Figure S20. ^{13}C-NMR spectrum of Au(I)-Hg(II) heterobimetallic complex **6a**.

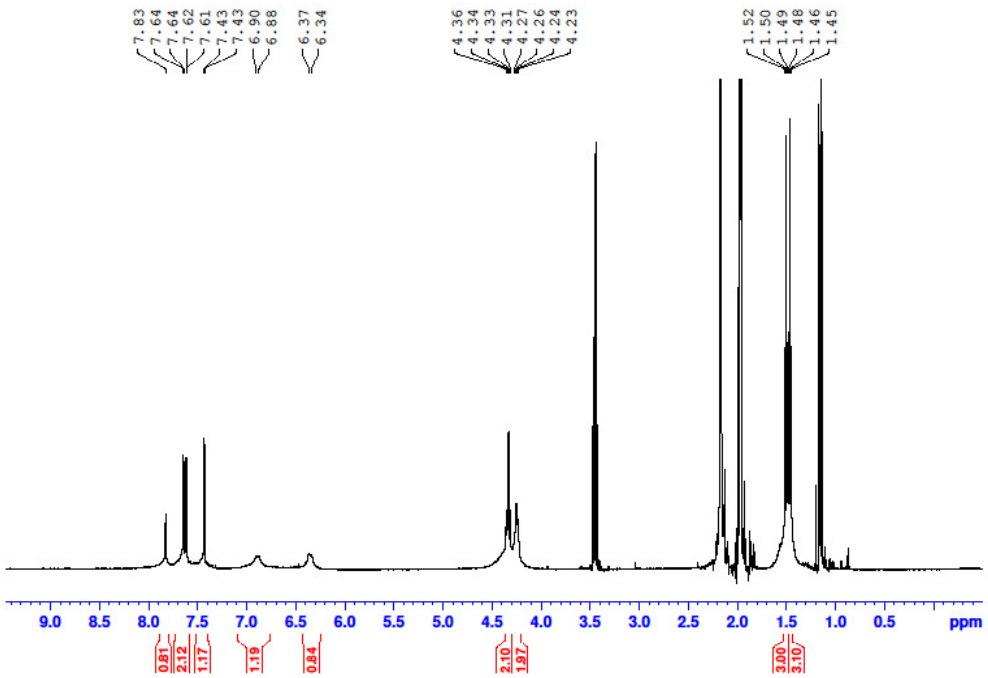

Figure S21. ^{1}H-NMR spectrum of Au(I)-Hg(II) heterobimetallic complex **6b**.

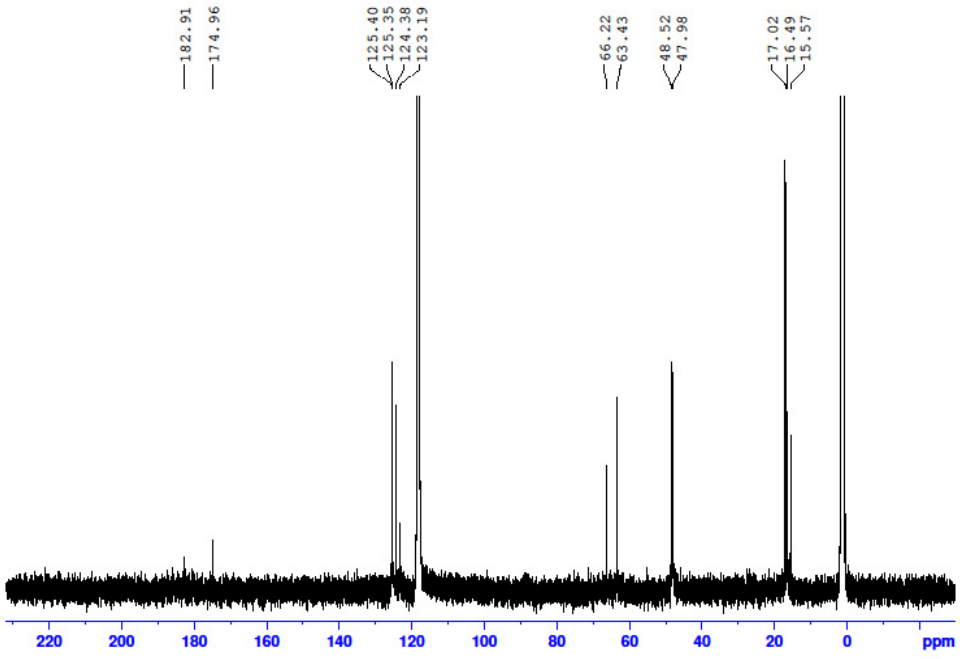

Figure S22. ^{13}C-NMR spectrum of Au(I)-Hg(II) heterobimetallic complex **6b**.

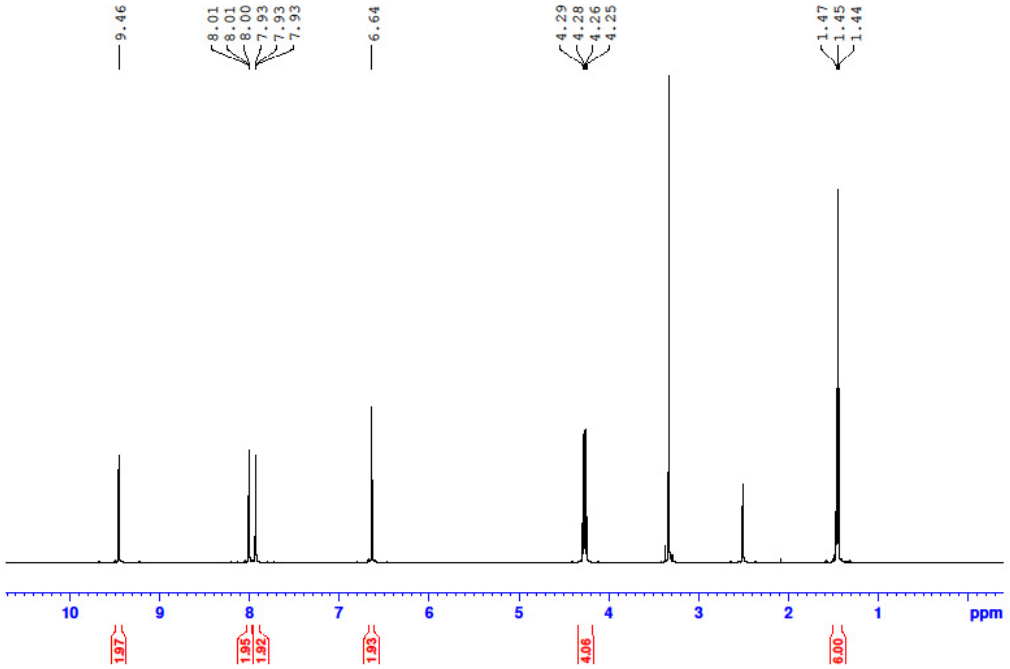

Figure S23. ^{1}H-NMR spectrum of *bis*-imidazolium pro-ligand **7**.

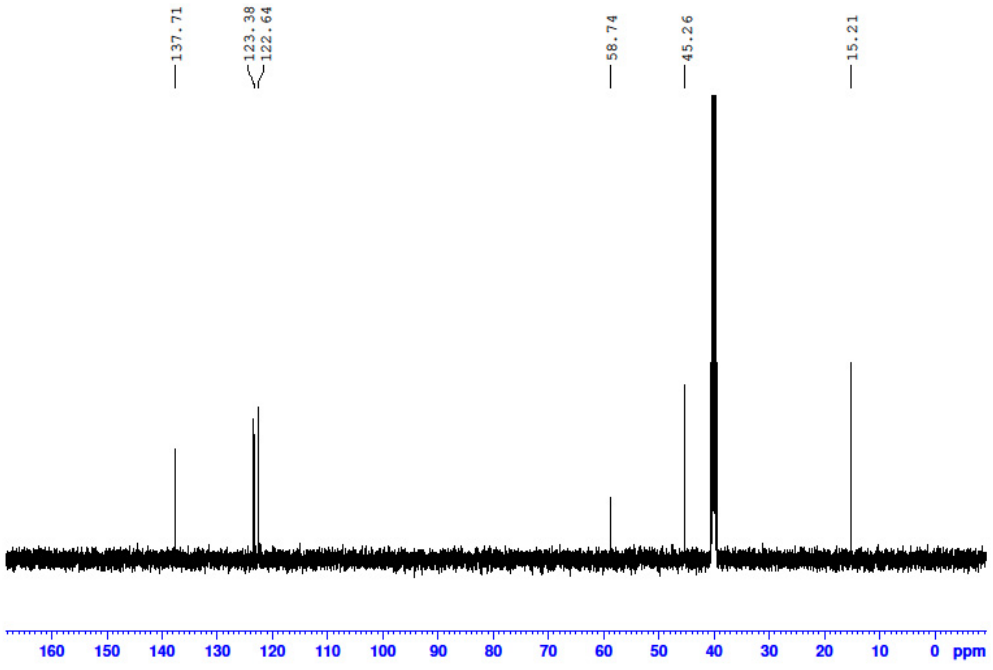

Figure S24. ^{13}C-NMR spectrum of *bis*-imidazolium pro-ligand **7**.

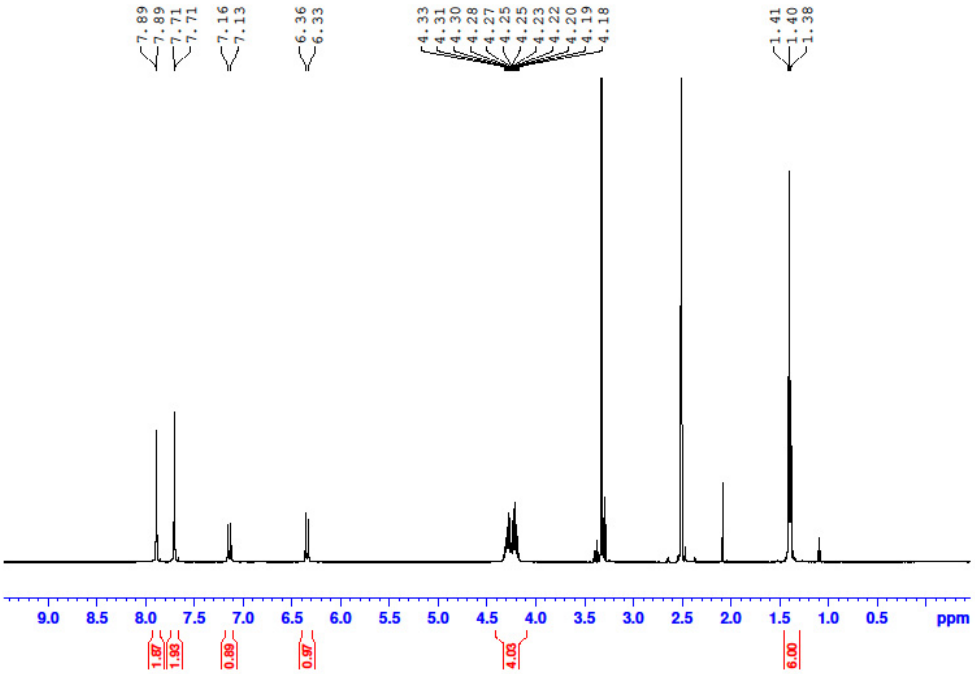

Figure S25. [1]H-NMR spectrum of Au(I) homobimetallic complex **8a**.

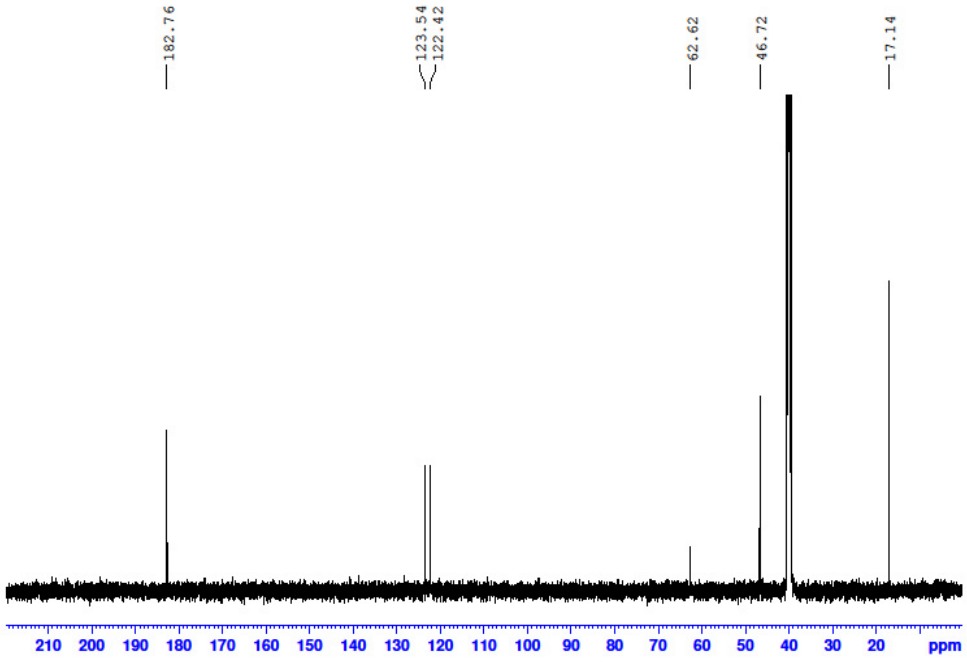

Figure S26. [13]C-NMR spectrum of Au(I) homobimetallic complex **8a**.

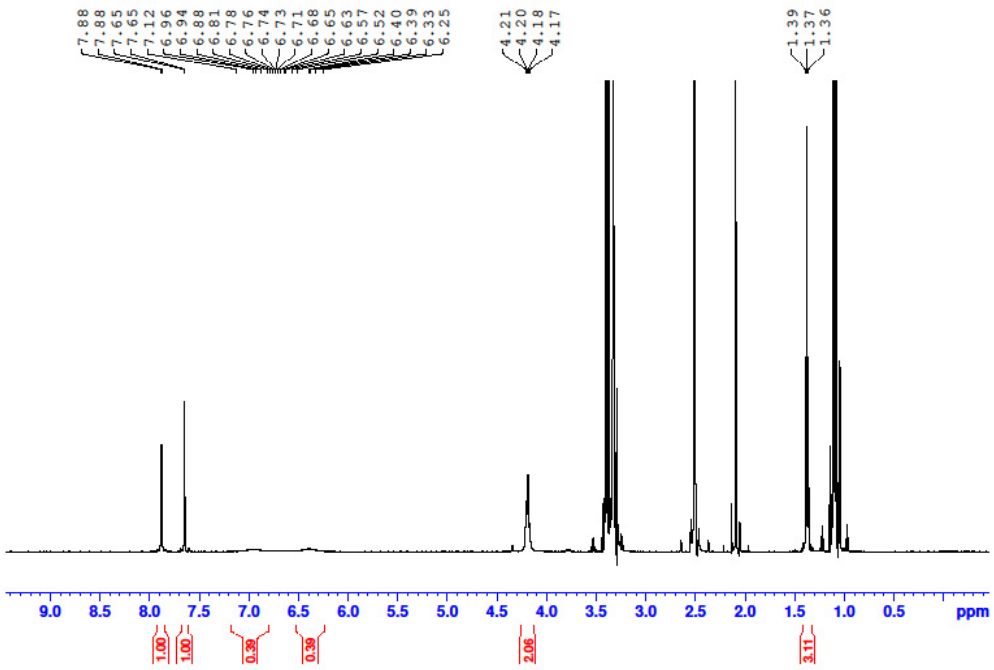

Figure S27. [1]H-NMR spectrum of Ag(I) homobimetallic complex **8b**.

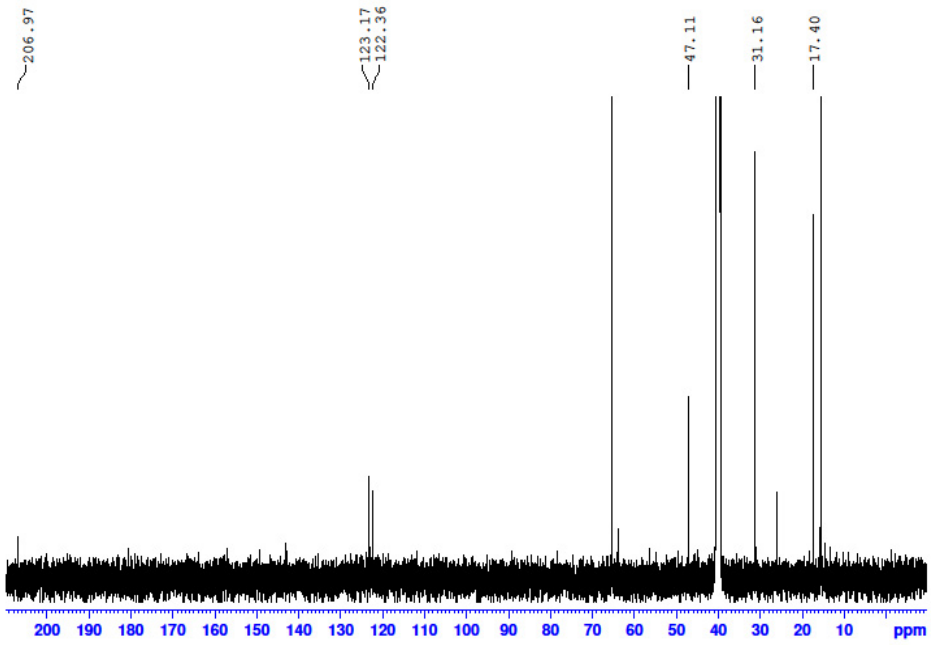

Figure S28. [13]C-NMR spectrum of Ag(I) homobimetallic complex **8b**.

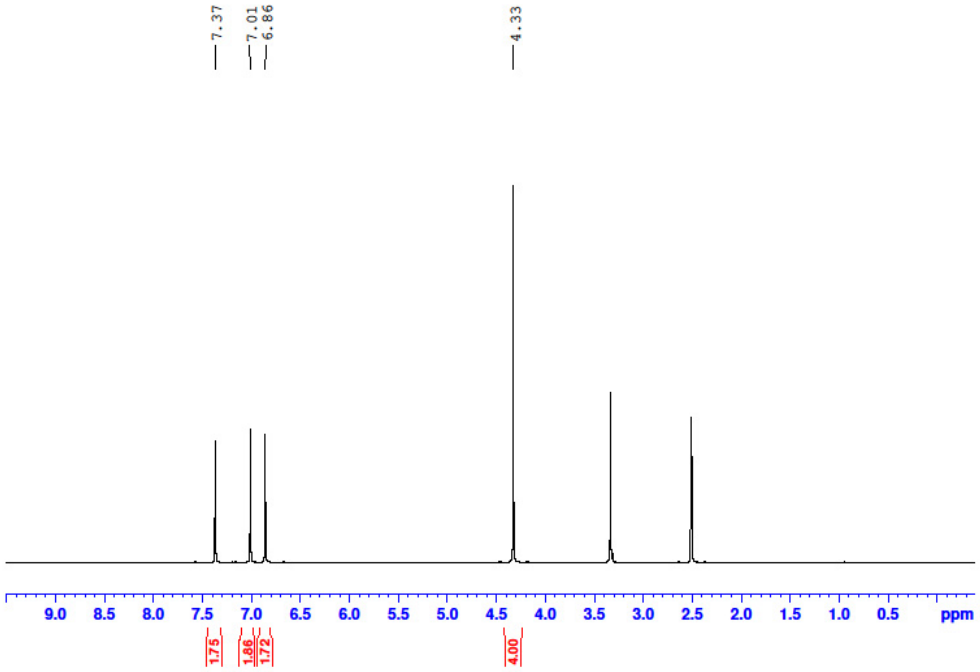

Figure S29. ^{1}H-NMR spectrum of compound **9**.

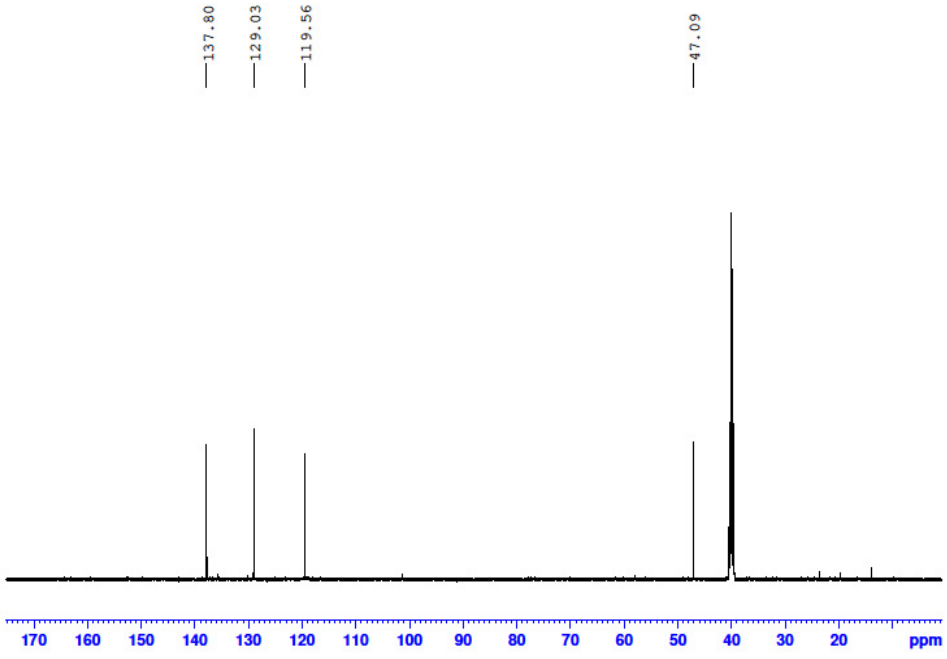

Figure S30. ^{13}C-NMR spectrum of compound **9**.

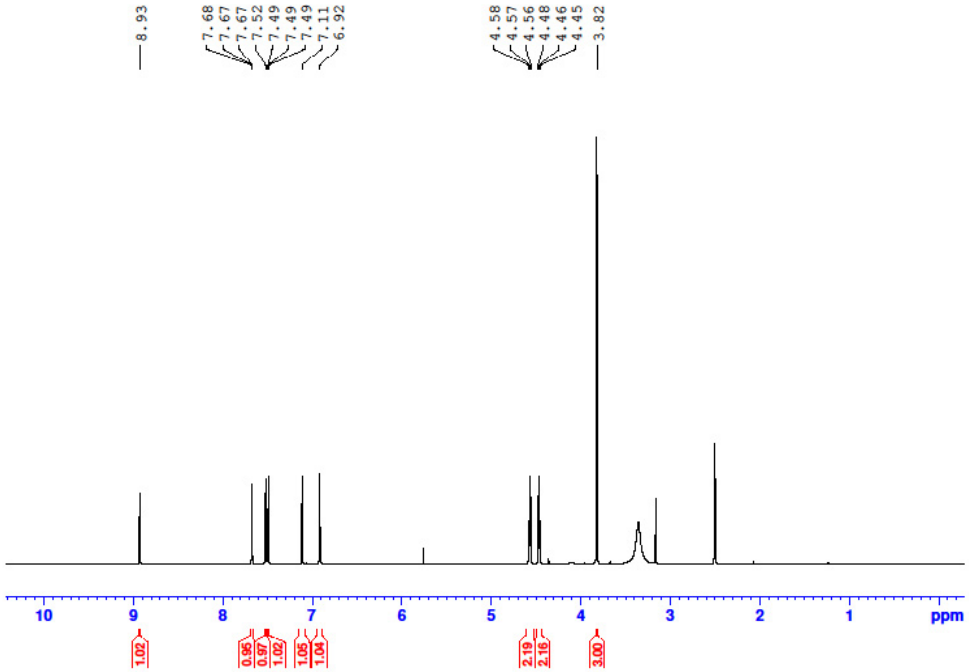

Figure S31. ^{1}H-NMR spectrum of pro-ligand **10a**.

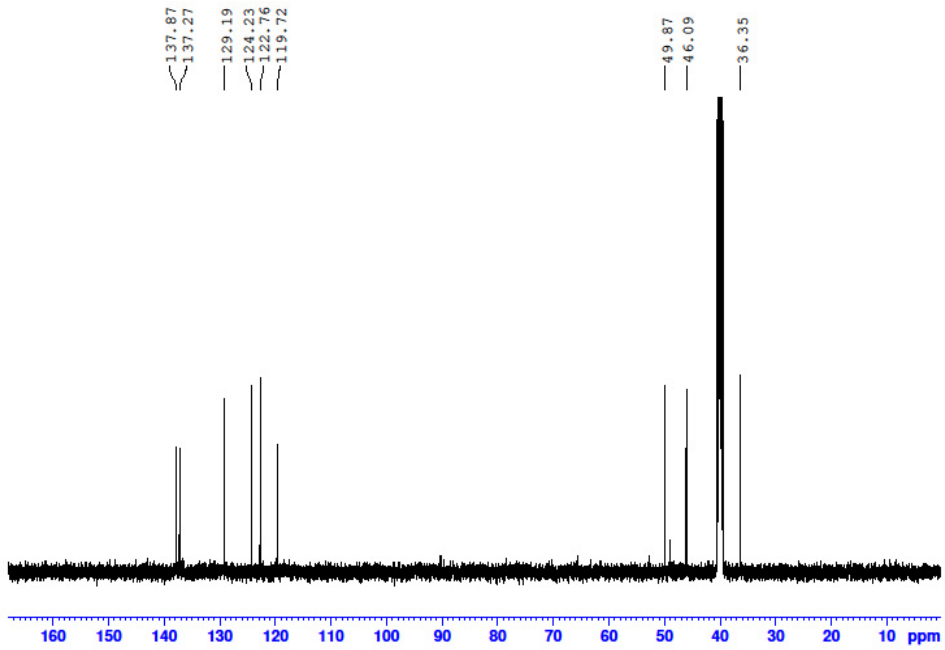

Figure S32. ^{13}C-NMR spectrum of pro-ligand **10a**.

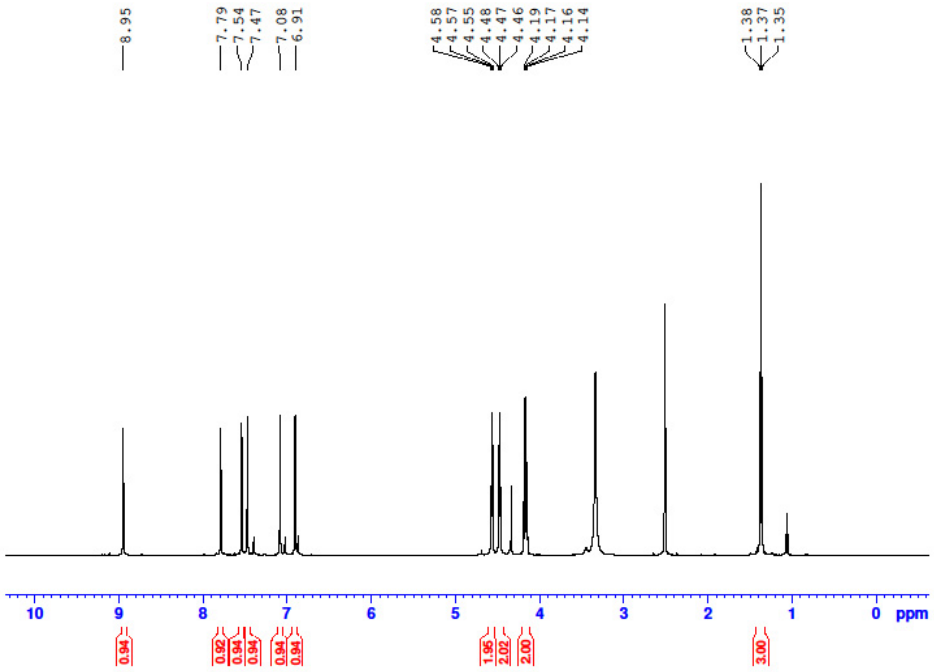

Figure S33. ^{1}H-NMR spectrum of pro-ligand **10b**.

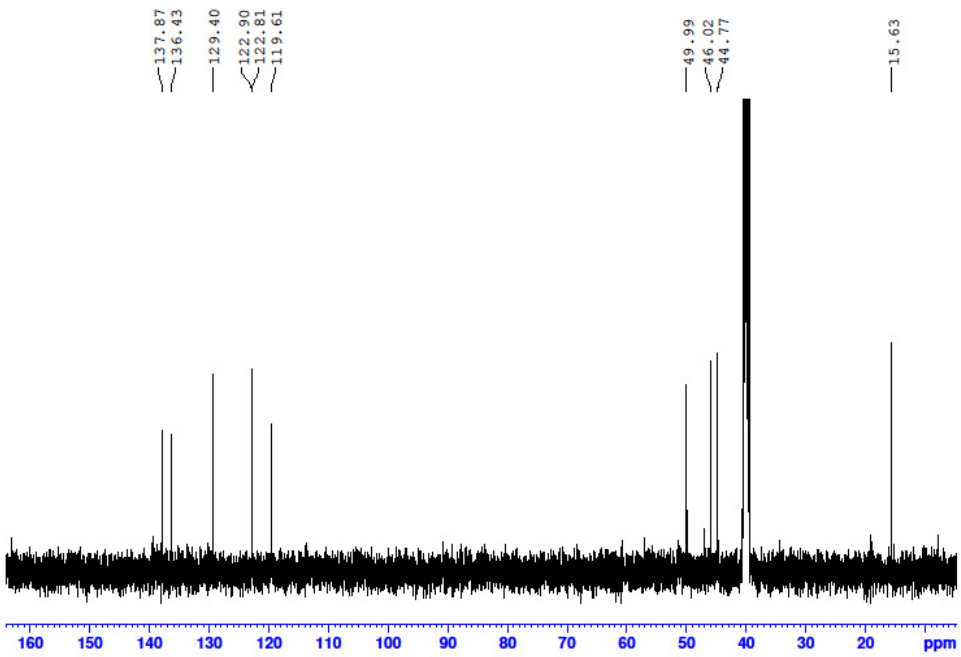

Figure S34. ^{13}C-NMR spectrum of pro-ligand **10b**.

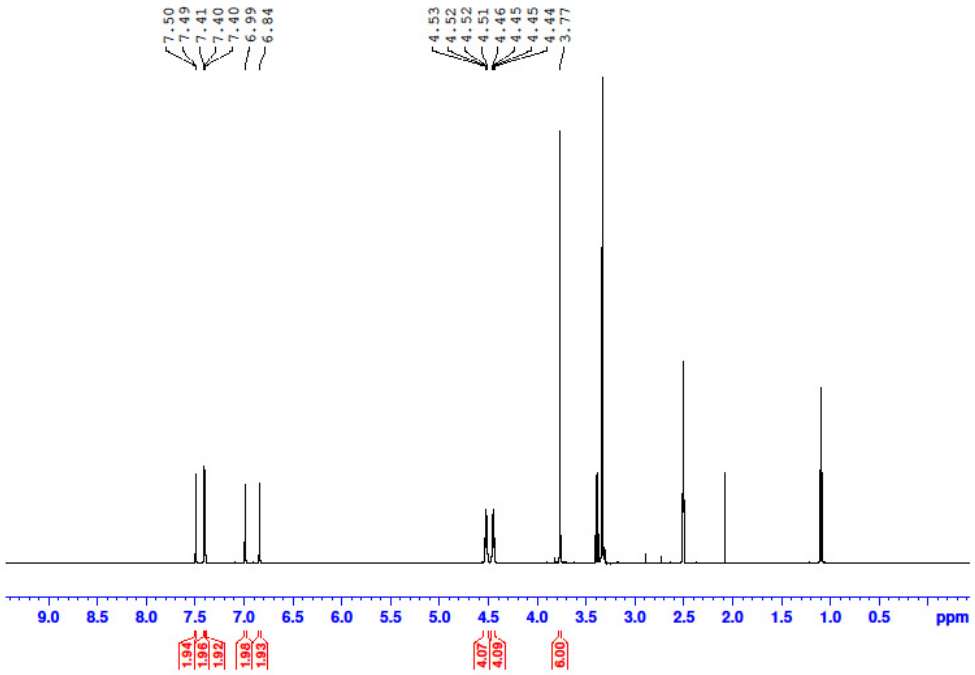

Figure S35. ^{1}H-NMR spectrum of Au(I) monometallic complex **11a**.

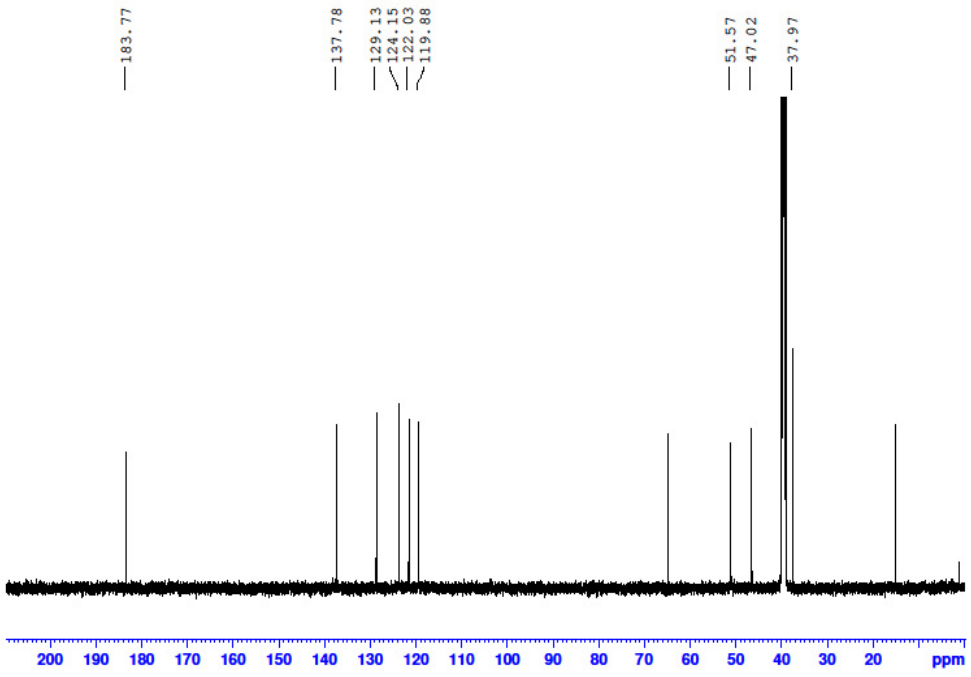

Figure S36. ^{13}C-NMR spectrum of Au(I) monometallic complex **11a**.

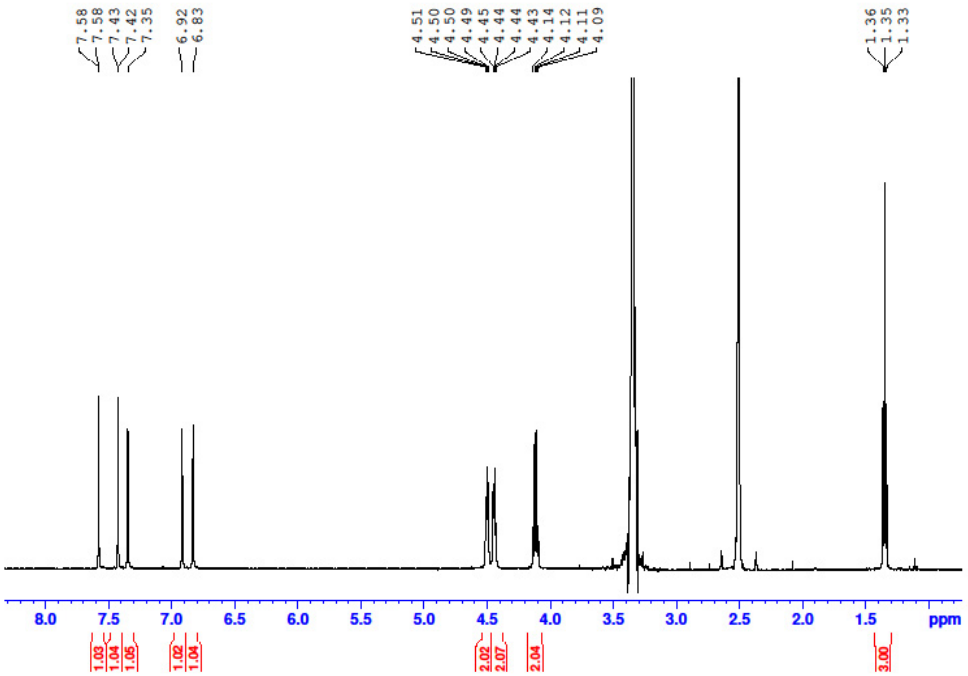

Figure S37. ^{1}H-NMR spectrum of Au(I) monometallic complex **11b**.

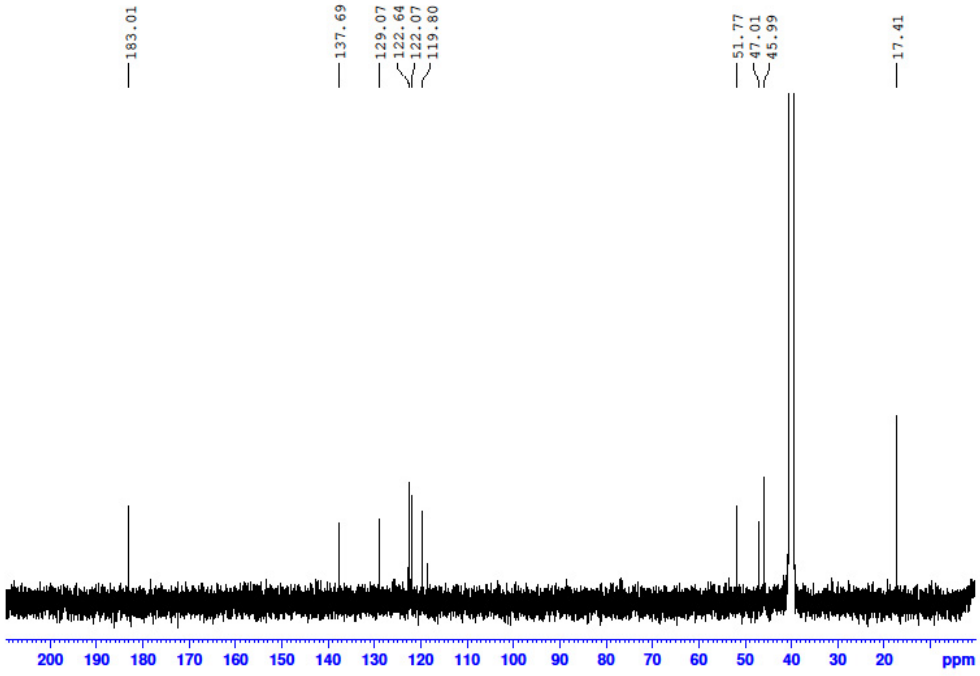

Figure S38. ^{13}C-NMR spectrum of Au(I) monometallic complex **11b**.

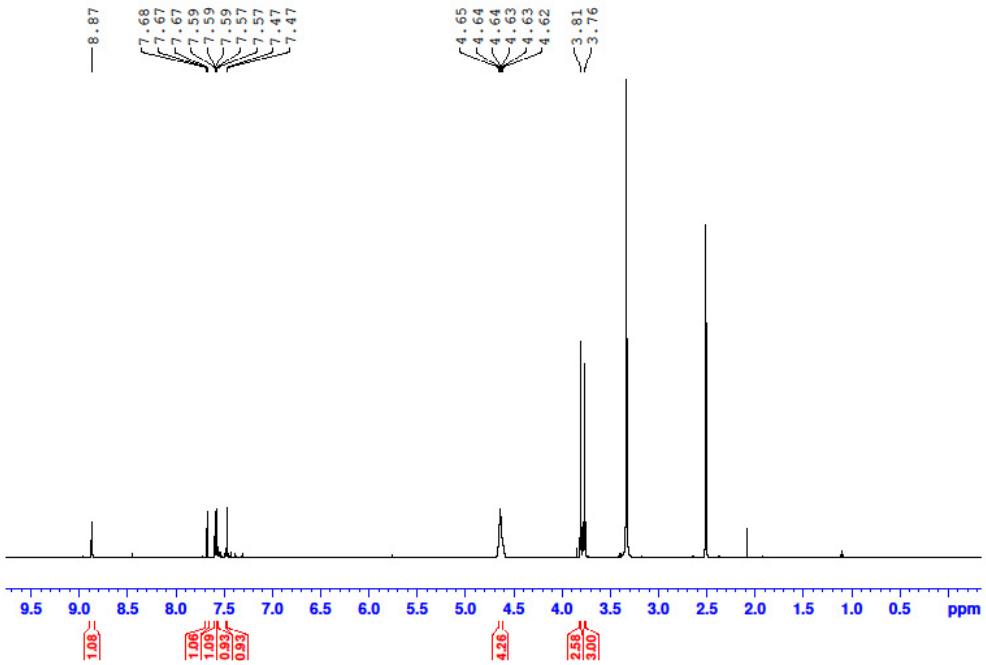

Figure S39. ^{1}H-NMR spectrum of Au(I) monometallic complex **12a**.

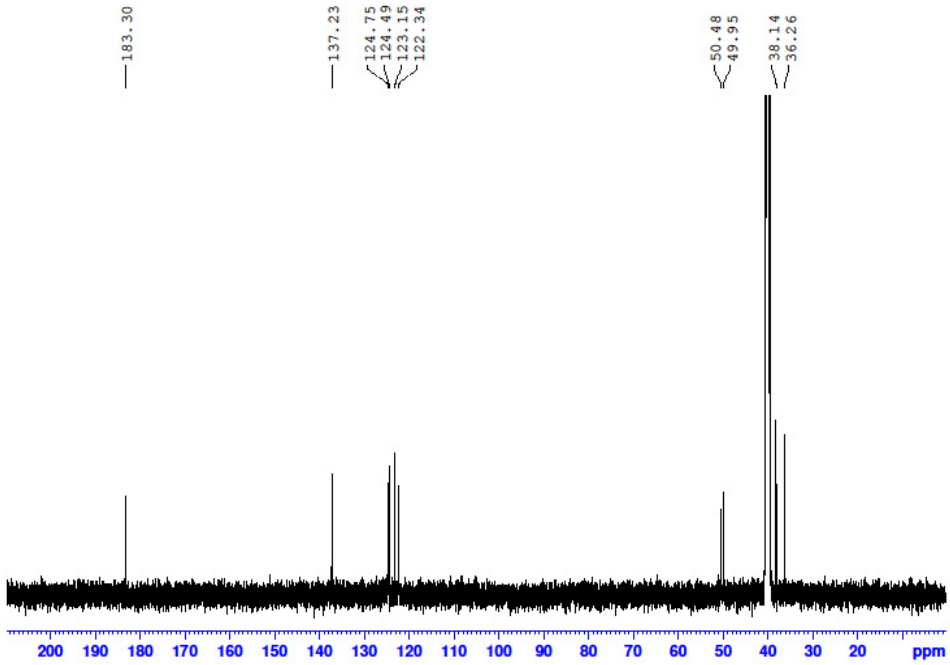

Figure S40. ^{13}C-NMR spectrum of Au(I) monometallic complex **12a**.

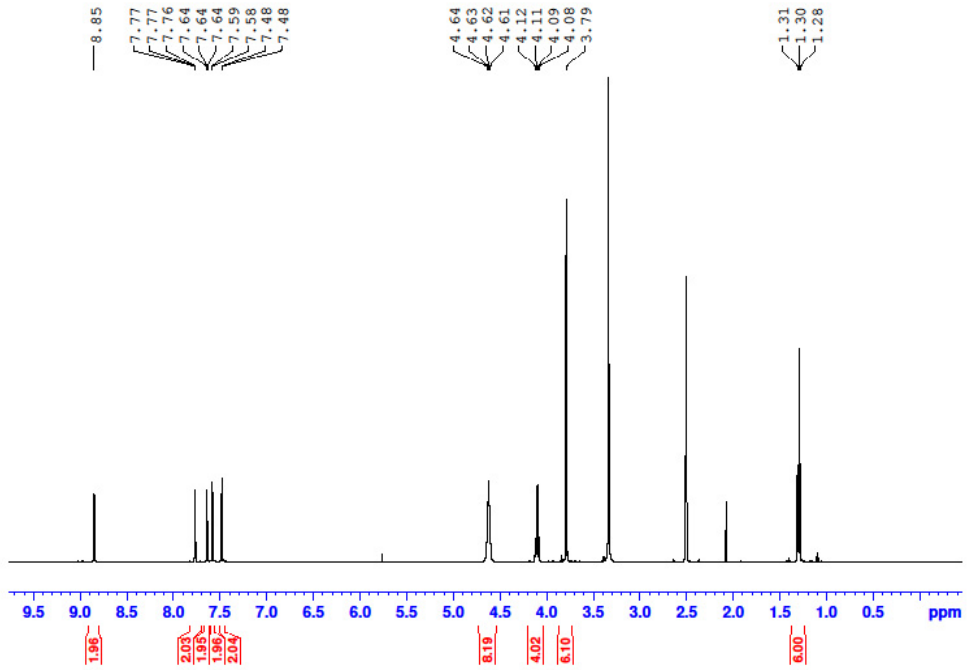

Figure S41. ^{1}H-NMR spectrum of Au(I) monometallic complex **12b**.

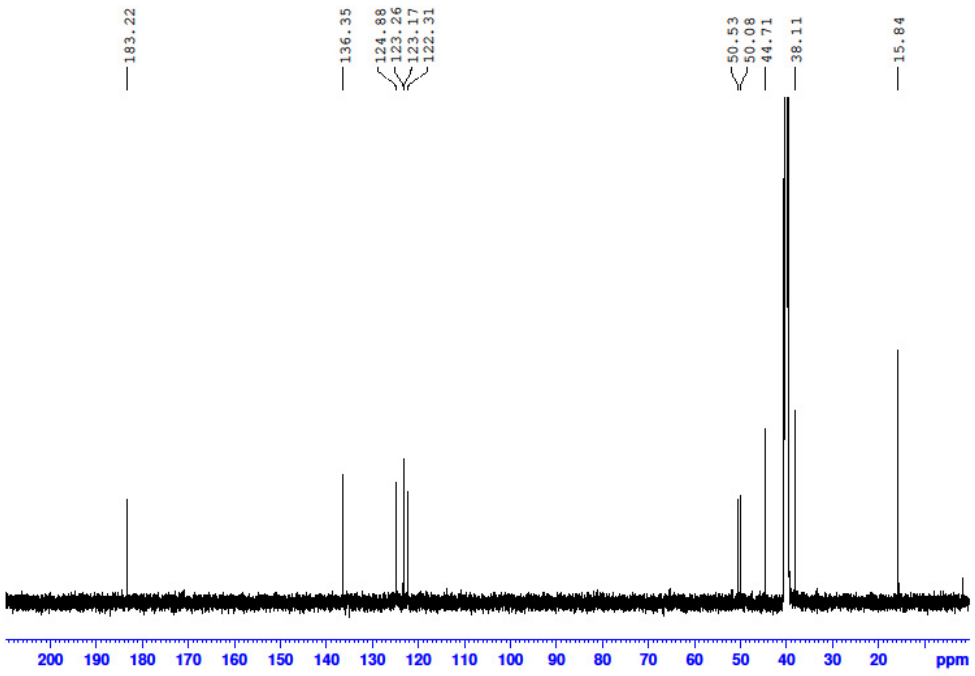

Figure S42. ^{13}C-NMR spectrum of Au(I) monometallic complex **12b**.

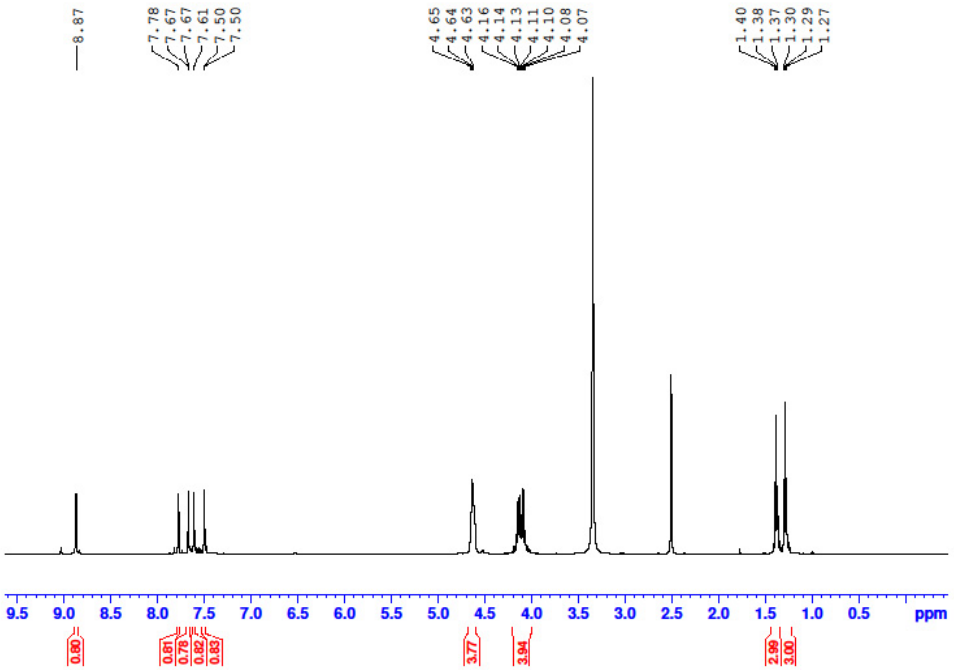

Figure S43. [1]H-NMR spectrum of Au(I) monometallic complex **12c**.

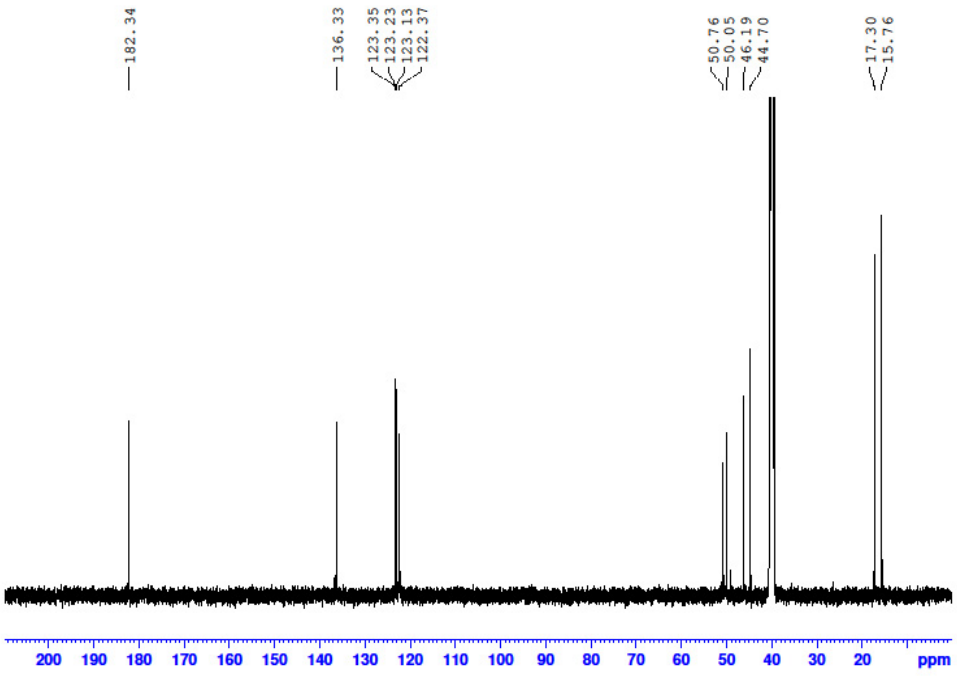

Figure S44. [13]C-NMR spectrum of Au(I) monometallic complex **12c**.

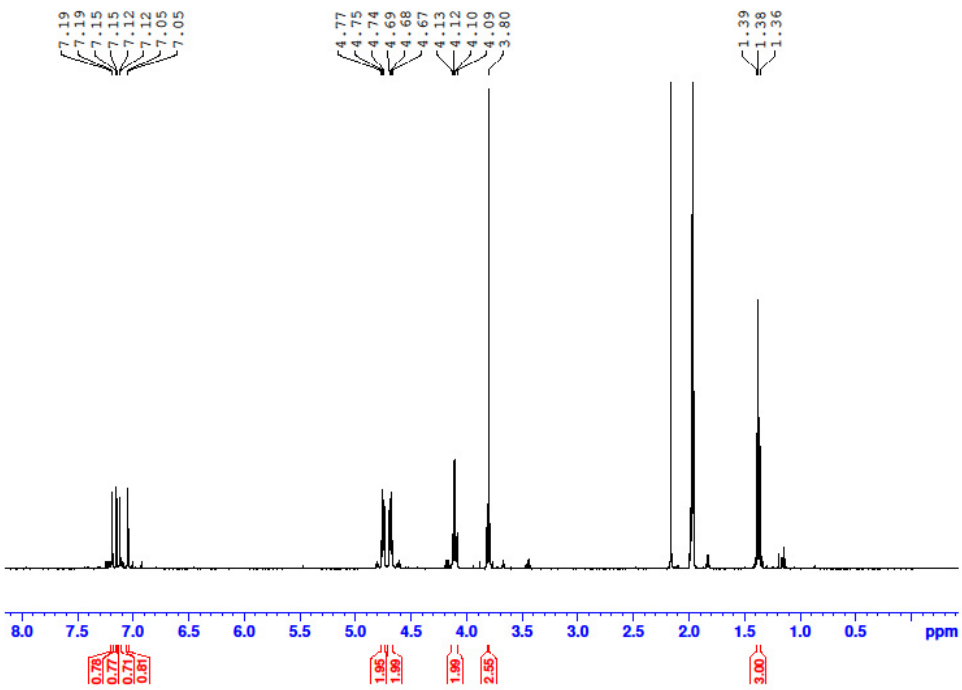

Figure S45. [1]H-NMR spectrum of Au(I)-Ag(I) heterometallic complex **13b**.

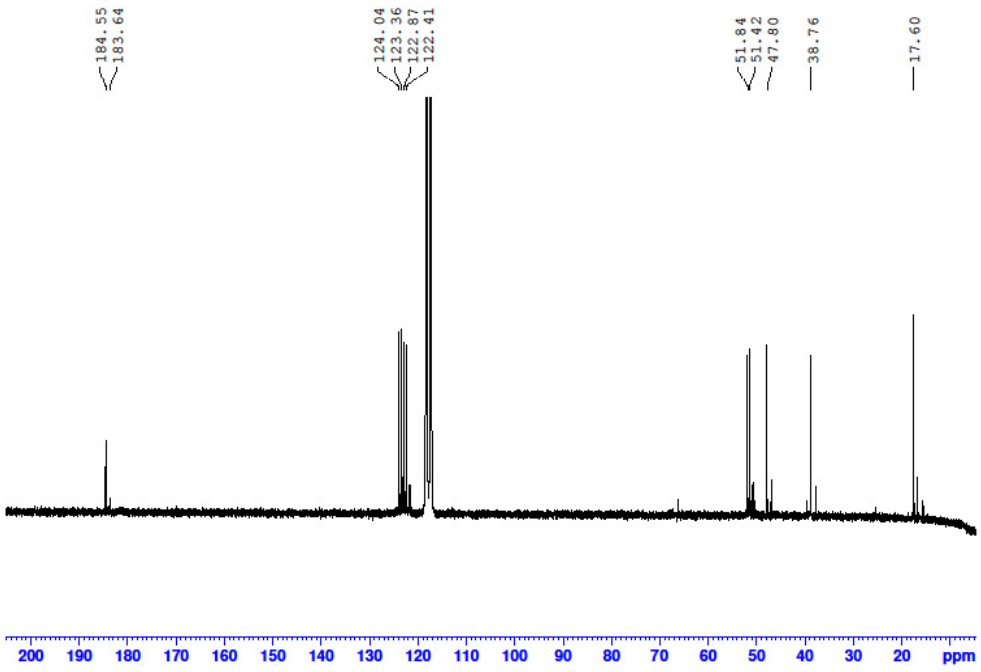

Figure S46. [13]C-NMR spectrum of Au(I)-Ag(I) heterometallic complex **13b**.

Variable temperature NMR studies

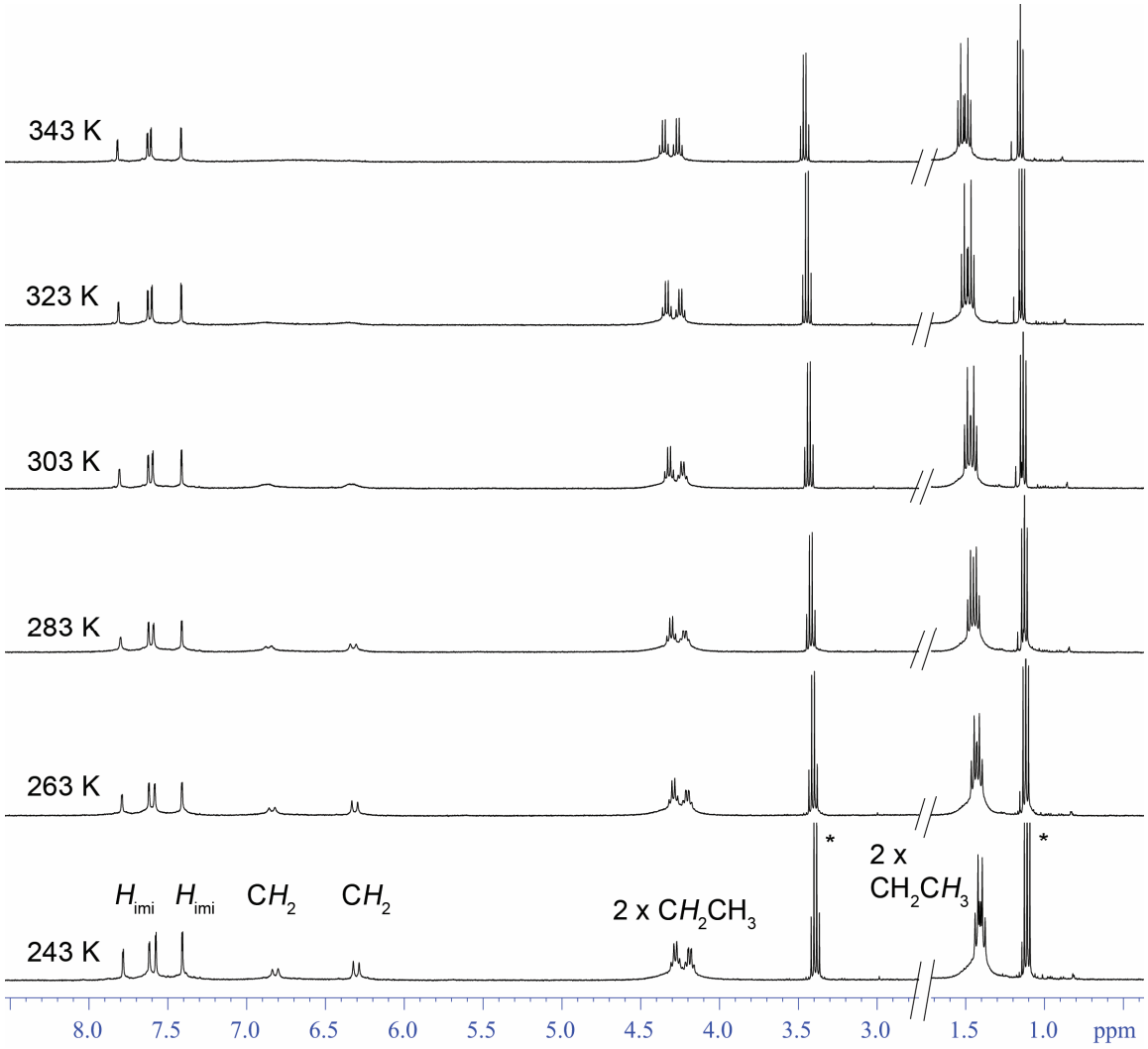

Figure S47. Stacked ^{1}H-NMR spectra of Au(I)-Hg(II) heterobimetallic complex **6b**.

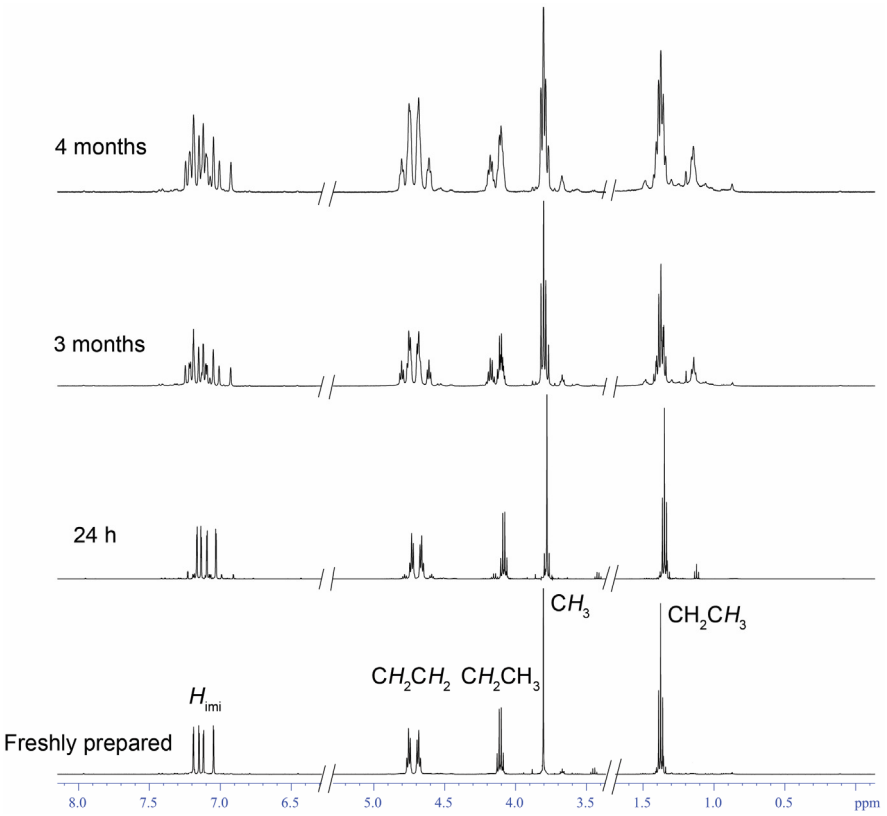

Figure S48. Time course ^{1}H NMR experiment showing the decomposition of compound **13b** over a period of 4 months in d$_3$-CD$_3$CN.

Mass Spectra

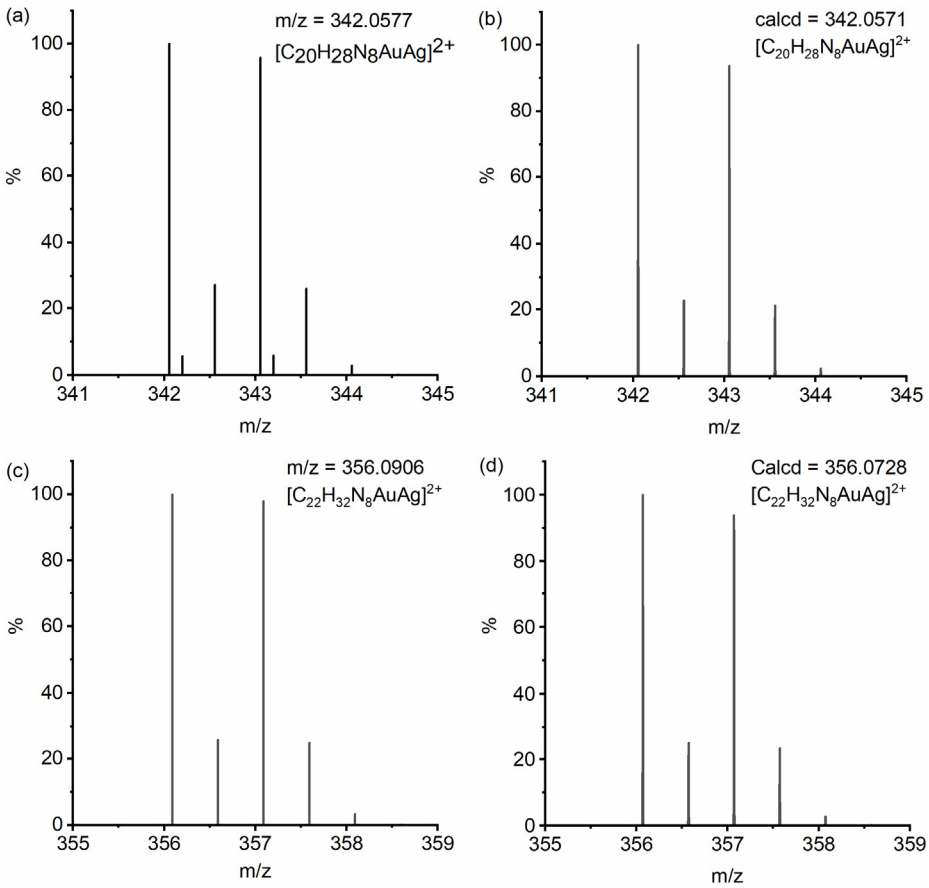

Figure S49. (a) High-resolution mass spectrum of Au(I)-Ag(I) heterobimetallic complex **5a** and (b) theoretical mass spectrum for isotopic distribution for $[C_{20}H_{28}N_8AuAg]^{2+}$ corresponding to **5a** and (c) High-resolution mass spectra for complex **5b** and (d) Theoretical mass spectrum for isotopic distribution for $[C_{22}H_{32}N_8AuAg]^{2+}$ corresponding to **5b**.

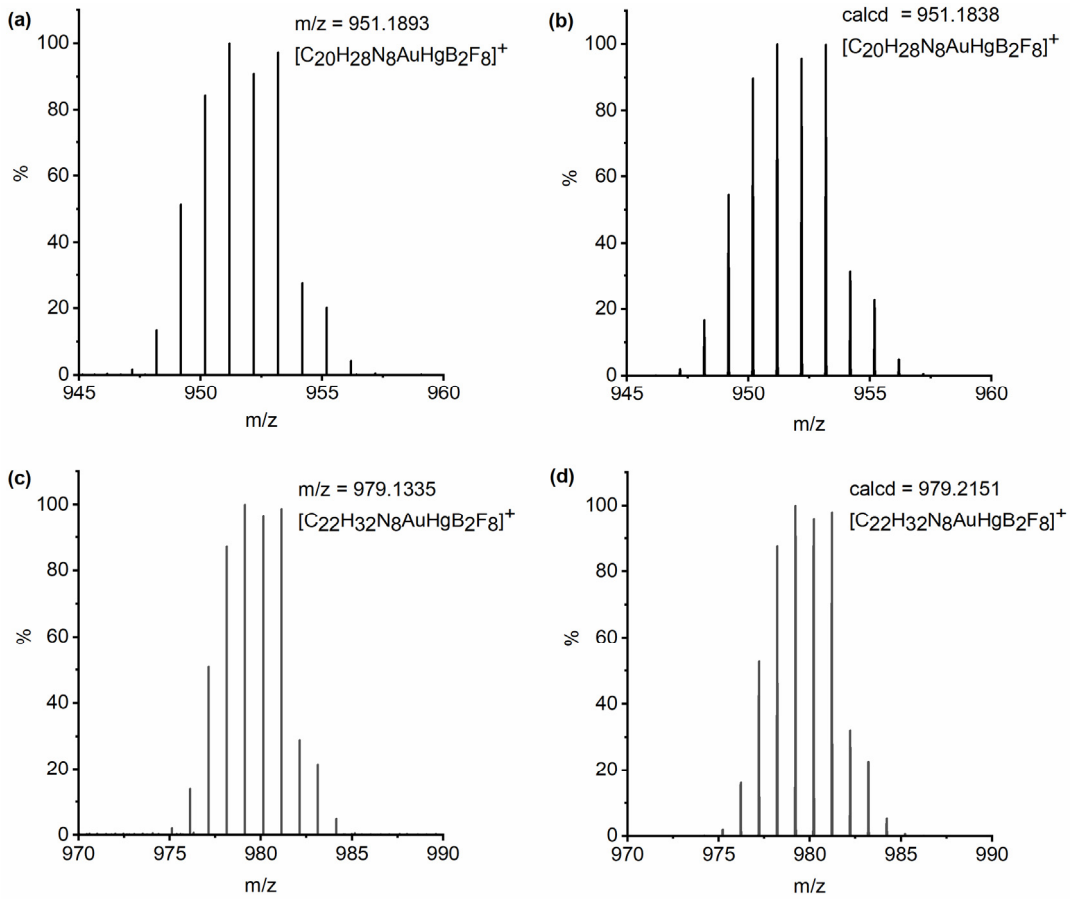

Figure S50. (a) High-resolution mass spectrum of Au(I)-Hg(II) heterobimetallic complex **6a** and (b) Theoretical mass spectrum showing isotopic distribution for $[C_{20}H_{28}N_8AuHgB_2F_8]^+$ corresponding to **6a** and (c) high-resolution mass spectrum of **6b** and (d) Theoretical mass spectrum showing isotopic distribution for $[C_{22}H_{32}N_8AuHgB_2F_8]^+$ corresponding to **6b**.

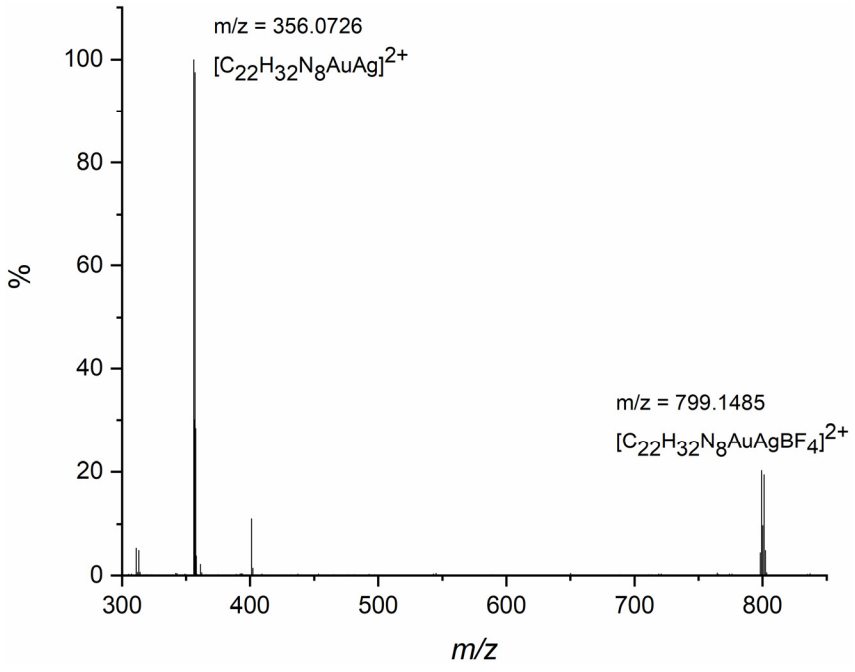

Figure S51. High-resolution mass spectrum of Au(I)-Ag(I) heterobimetallic complex **13b**.

Table S1. Crystallographic data for compounds **5b**, **8b**, **10a**, **11b**

	5b	**8b**	**10a**	**11b**
Empirical formula	$C_{20}H_{26}AgAuB_2F_8N_8$	$C_{22}H_{32}Ag_2B_2F_8N_8$	$C_9H_{13}N_4I$	$C_{20}H_{29}AuBr_2N_8$
Formula weight	856.94	797.91	304.14	738.30
Temperature/K	149.99(10)	150.00(10)	133.0(4)	149.98(10)
Crystal system	monoclinic	triclinic	monoclinic	triclinic
Space group	I2/a	P-1	$P2_1/c$	P-1
a/Å	13.49130(10)	8.72610(10)	6.8428(6)	10.7465(2)
b/Å	14.38060(10)	9.47660(10)	11.5230(5)	11.46525(18)
c/Å	17.91910(10)	9.62530(10)	17.2878(15)	12.0732(2)
α/°	90	82.3560(10)	90	65.8087(16)
β/°	106.4520(10)	67.8470(10)	124.136(12)	85.8739(15)
γ/°	90	85.3190(10)	90	80.8541(15)
Volume/Å^3	3334.20(4)	730.216(15)	1128.3(2)	1339.64(4)
Z	4	1	2	2
ρ_{calc}g/cm^3	1.707	1.814	1.790	1.830
μ/mm^{-1}	13.480	11.483	22.055	13.989
F(000)	1640.0	396.0	592.0	708.0
Crystal size/mm^3	0.04 × 0.04 × 0.02	0.07 × 0.06 × 0.04	0.04 × 0.02 × 0.02	0.08 × 0.05 × 0.03
Radiation	CuKα (λ = 1.54184)	CuKα (λ = 1.54184)	CuKα (λ = 1.54184)	CuKα (λ = 1.54184)
2Θ range for data collection/°	8.016 to 142.512	9.422 to 136.784	9.856 to 148.96	8.028 to 142.452
Index ranges	-15 ≤ h ≤ 16, -17 ≤ k ≤ 17, -21 ≤ l ≤ 17	-10 ≤ h ≤ 10, -11 ≤ k ≤ 11, -11 ≤ l ≤ 11	-8 ≤ h ≤ 8, -14 ≤ k ≤ 14, -21 ≤ l ≤ 21	-13 ≤ h ≤ 13, -14 ≤ k ≤ 12, -14 ≤ l ≤ 11
Reflections collected	33825	24497	9270	28172
Independent reflections	3241 [R_{int} = 0.0279, R_{sigma} = 0.0094]	2681 [R_{int} = 0.0586, R_{sigma} = 0.0188]	2315 [R_{int} = 0.0333, R_{sigma} = 0.0234]	5174 [R_{int} = 0.0289, R_{sigma} = 0.0154]
Data/restraints/parameters	3241/2/201	2681/0/192	2315/0/128	5174/225/283
Goodness-of-fit on F^2	1.084	1.114	1.086	1.044
Final R indexes [I>=2σ (I)]	R_1 = 0.0217, wR_2 = 0.0593	R_1 = 0.0266, wR_2 = 0.0702	R_1 = 0.0303, wR_2 = 0.0846	R_1 = 0.0347, wR_2 = 0.0932
Final R indexes [all data]	R_1 = 0.0220, wR_2 = 0.0595	R_1 = 0.0266, wR_2 = 0.0702	R_1 = 0.0331, wR_2 = 0.0888	R_1 = 0.0351, wR_2 = 0.0935
Largest diff. peak/hole / e Å^{-3}	0.62/-0.54	0.67/-1.18	0.62/-1.37	1.64/-1.66

Further X-ray Crystallographic details

5b. Solved in the monoclinic space group I2/a. The structure contains disordered diethyl ether solvent molecules at partial occupancy. A satisfactory disorder model for the solvent could not be found, and therefore the OLEX2 Solvent Mask routine was used to mask out the disordered density. The total solvent accessible volume / cell = 637.0 Ang^3 [19.1%], with a total electron count / cell = 162.2. This corresponds to ~3.9 diethyl ether molecules / cell.

11b. Solved in the triclinic space group P-1. The structure contains a disordered water molecule at partial occupancy and attempts to model this disorder using two different closely spaced positions were unsatisfactory with the site occupancy for one component refining to unreasonably low levels.

As a result, the OLEX2 Solvent Mask routine was used to mask out the disordered density. The total solvent accessible volume / cell = 114.9 Ang^3 [8.6%], with a total electron count / cell = 30.9. This corresponds to ~3 water molecules / cell.

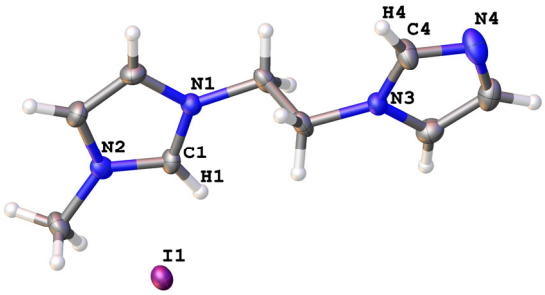

Figure S52. Representation of the X-ray crystal structure of **10a**. Atomic displacement ellipsoids are shown at the 50% probability level.

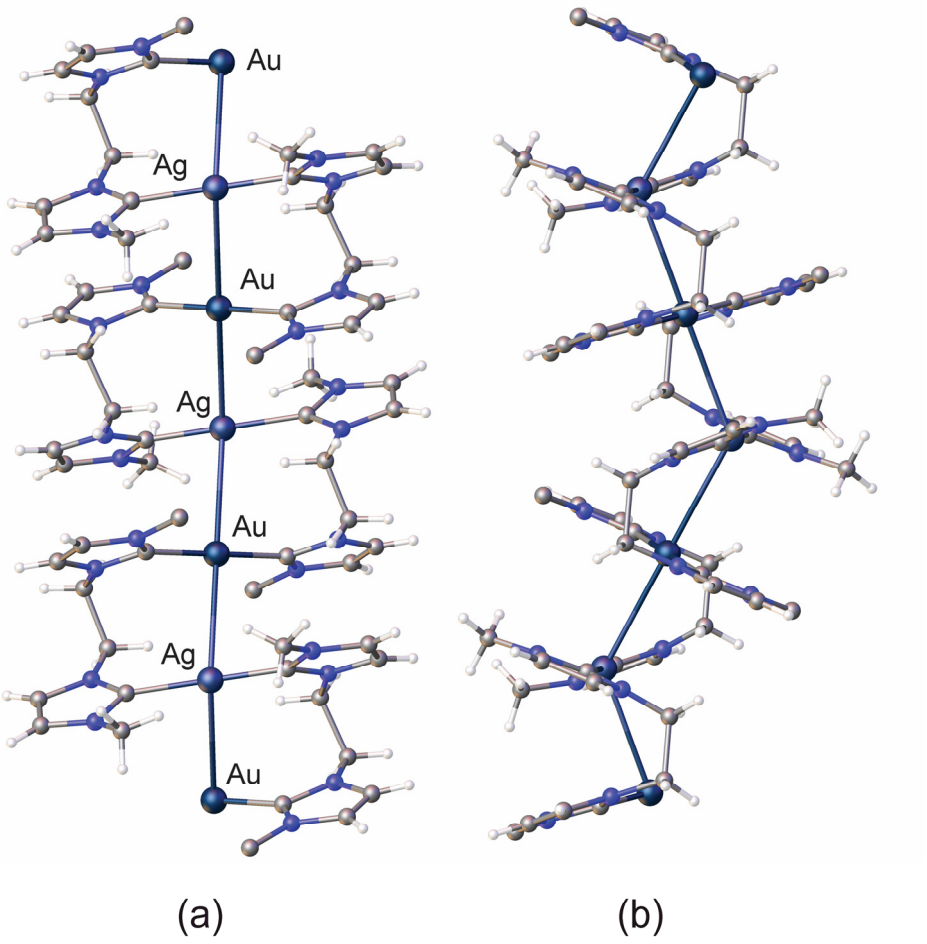

Figure S53. Two representation of the poor-quality crystal structure obtained from the ^{1}H NMR decomposition experiment for compound **13b** showing the coordination polymeric structure of the product. The tetrafluoroborate counterions have been omitted for clarity.

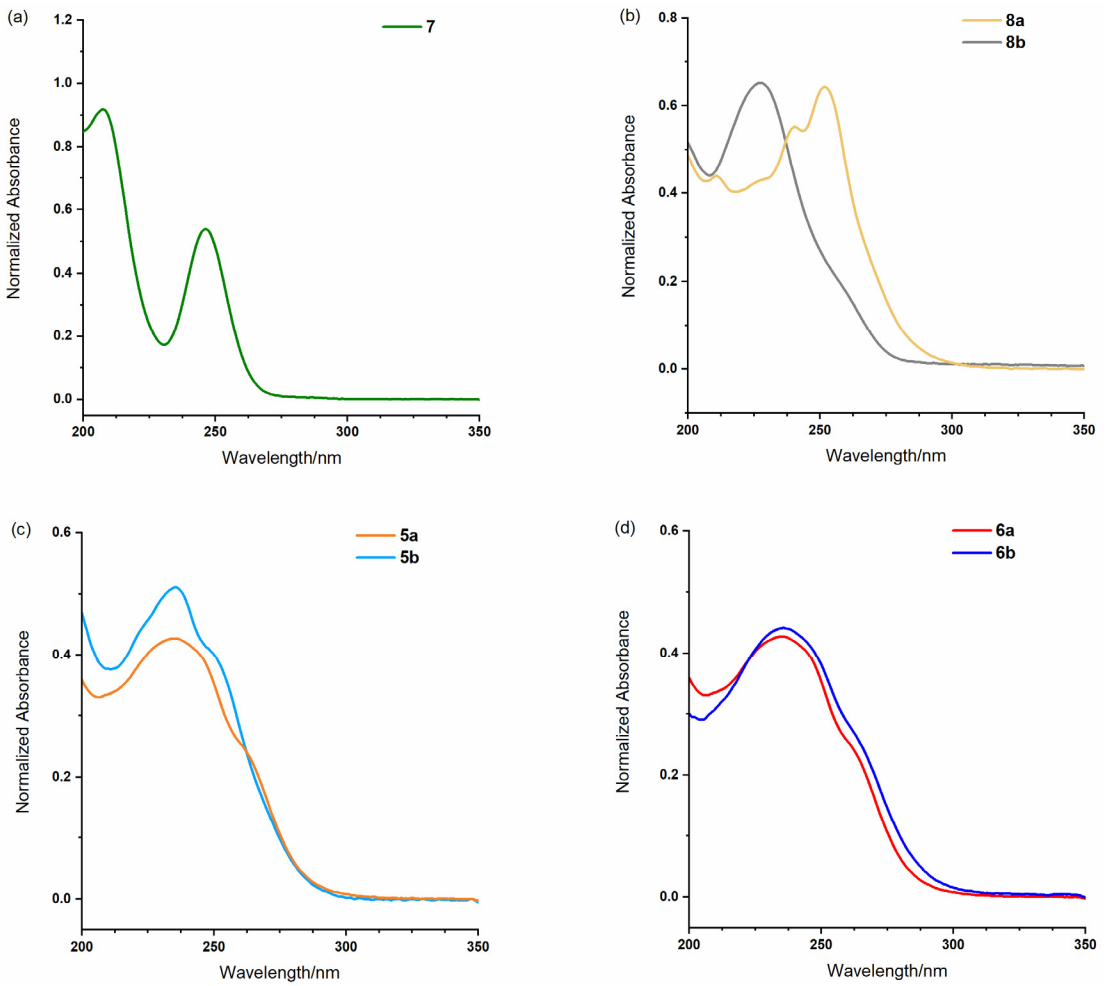

Figure S54. UV-vis spectra of (a) **7** and (b) homobimetallic complexes **8a** and **8b** and (c) Au(I)-Ag(I) heterobimetallic complexes **5a** and **5b** and (d) Au(I)-Hg(II) heterobimetallic complexes **6a** and **6b**. All the spectra were recorded at 2.0×10^{-5} M from acetonitrile solutions.

Table S2. Spectroscopic properties of **5a**, **5b**, **6a**, **6b**, **7**, **8a**, and **8b**.

	UV-vis λ_{max}/nm (ε/M^{-1}·cm^{-1})
7	208 (40703), 246 (25796)
5a	237 (23969), 254 (17109)
5b	235 (18439), 251 (12240)
6a	237(14961), 261(13773)
6b	237 (22057), 263 (12961)
8a	211(16240), 228 (210847), 240 (27589), 252 (32228)
8b	228 (32828), 258 (9879)

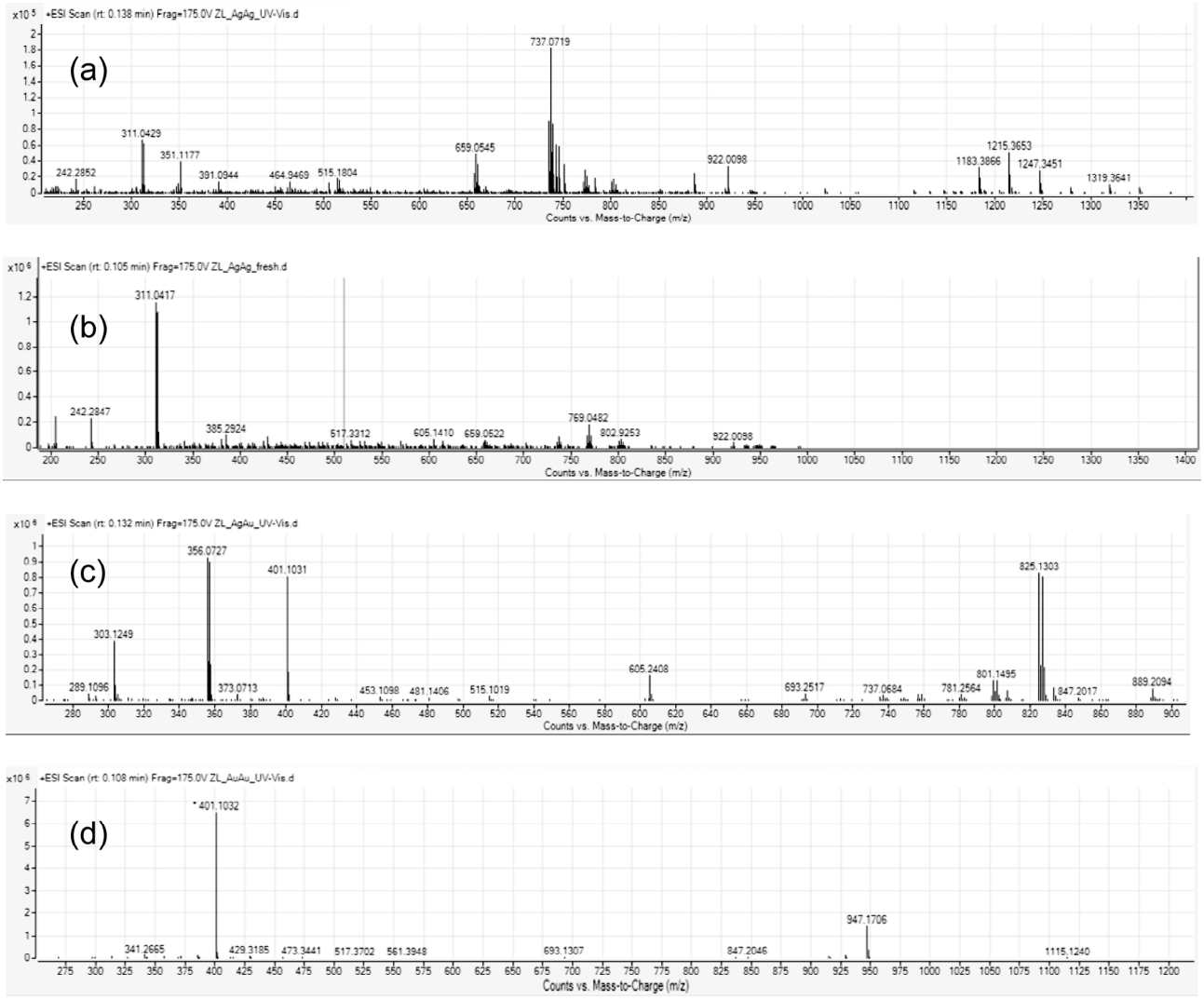

Figure S55. High-resolution mass spectra obtained from solutions (10% CH_3CN, 90% H_2O) of (a) 8b (b) 8b (freshly prepared in CH_3CN) (c) 5b and (d) 8a at the conclusion (48 h) of a stability study experiment.

Table S3. Minimum inhibitory concentration (MIC, μM) values for compounds **7**, **8a**, **8b**, **5a** and **5b**.

Compound	Gram-positive		Gram-negative	
	E. faecium[a]	*S. aureus*[b]	*A. baumannii*[c]	*E. coli*[d]
7	>556	>556	>556	>556
8a	>262	>262	>262	>262
8b	20	40	10	33 ± 7
5a	12 ± 3	25 ± 6	6 ± 2	18
5b	9	18	6 ± 2	15 ± 3

[a]*E. faecium* ATCC BAA-2127, [b]*S. aureus* ATCC 9144™, [c]*A. baumannii* ATCC 17978™, and [d]*E. coli* ATCC BAA-2340™

References

1. A. Fernández, M. López-Torres, J. J. Fernández, D. Vázquez-García and I. Marcos, *J. Chem. Educ.*, 2017, **94**, 1552-1556.
2. S. Kobialka, C. Müller-Tautges, M. T. S. Schmidt, G. Schnakenburg, O. Hollóczki, B. Kirchner and M. Engeser, *Inorg. Chem.*, 2015, **54**, 6100-6111.